



# Non-precious metal-modified sensors for nitrite detection

Yu-Xi Yang<sup>1,2</sup> · Tingting Zhang<sup>1,2</sup> · Jie Zhang<sup>1,2</sup> · Jing-He Yang<sup>3</sup>

Received: 30 June 2023 / Revised: 1 August 2023 / Accepted: 15 August 2023 / Published online: 24 August 2023  
© The Author(s), under exclusive licence to Springer-Verlag GmbH Germany, part of Springer Nature 2023

## Abstract

Nitrite is widely used due to its personal properties. It not only exists in the food processing and chemical industry but also in every corner of the natural world. Nevertheless, excessive use of nitrite can cause serious environmental and human health hazards. Therefore, the efficient and sensitive detection of nitrite content has become a problem that must be faced. Among numerous methods, the electrochemical method has been widely studied for its advantages, such as fast reaction speed, high sensitivity, and miniaturization. The principle of operation of the nitrite electrochemical sensor is as follows. A modified layer located on the electrode surface oxidizes nitrite to nitrate. The sensing signal generated during oxidation can be converted into a measurable electrochemical signal. The electrochemical signal is proportional to nitrite concentration within a certain range, so that nitrite can be quantitatively detected. However, the sensor's performance is affected by the high oxidation potential of the bare electrode in electrochemistry. Therefore, the electrode is often modified to improve the sensor's performance in the study. In this review, the research progress of materials other than precious metals is discussed in the electrochemical detection of nitrite in recent years (2023–2013). The properties of carbon materials, non-noble metals, metal-organic framework compounds, conductive polymers, and their composites in electrochemical sensors are discussed in detail. Besides, it also looks forward to the challenges and prospects of nanomaterials in electrochemical sensor applications.

**Keywords** Non-precious metal · Composite materials · Nitrite · Electrochemical sensor

## Introduction

Nitrite is a nitrogenous compound that is ubiquitous in nature. It is mainly derived from the nitrogen cycle in nature. It is not only present in the environment but also widely used in the food processing and chemical industries [1]. It can be used in dye production in the chemical industry and certain organic synthesis, while it can be used as a food colorant and preservative in food production. However, when nitrite levels are too high, there is a greater risk to human

health and aquatic plants. On the one hand, when the nitrite concentration exceeds 0.02 mg/L, it will directly affect the growth and development of aquatic organisms, will induce disease outbreaks, and may even lead to the death of many aquatic organisms [2]. On the other hand, nitrite can form nitrosamines in the human body. Nitrosamines are precursors of carcinogenic compounds, and long-term ingestion can induce the development of cancer [3, 4]. The International Agency for Research on Cancer has classified nitrite as a possible carcinogen to humans (class 2a) [5]. At present, most countries have enacted corresponding laws and regulations to control the content of nitrite, which can reduce the harm of nitrite to humans and the environment to some extent. However, we still need to establish a complete testing program. A complete detection procedure is established when a systematic understanding of the mechanism of action nitrite is available [6].

At present, a variety of methods have been developed for the detection of nitrite content to control the excessive intake of nitrite content. Studies have been reported in the literature, and it has been found that the methods used include spectrophotometry [7, 8], chemiluminescence

✉ Jie Zhang  
zhangjie630@zzu.edu.cn

✉ Jing-He Yang  
jhyang@zzu.edu.cn

<sup>1</sup> School of Ecology and Environment, Zhengzhou University, Zhengzhou 450001, China

<sup>2</sup> Henan International Joint Laboratory of Environment and Resources, Zhengzhou University, Zhengzhou 450001, People's Republic of China

<sup>3</sup> School of Chemical Engineering, Zhengzhou University, Zhengzhou 450001, China

[9, 10], chromatography [11, 12], capillary electrophoresis [13–15], fluorescent probes [16], and electrochemistry [17]. Among the known methods, the electrochemical method has attracted wide attention because of its advantages of high sensitivity, simplicity, and accuracy.

In electrochemical detection, the electrochemical sensor is the most important component. The principle is that nitrite interacts with the material and thus undergoes a specific redox reaction at the electrode surface. The electrochemical active substances are produced during the reaction. And the substances can be converted into a detectable electrochemical signal by the sensor, thus being used for qualitative and quantitative analysis [18, 19]. The electrochemical method can realize direct electrocatalytic oxidation of nitrite on the electrode surface. However, the sensor's performance is hindered by the high oxidation potential of nitrite at the bare electrode [20]. Therefore, the electrode needs to be modified to improve the detection performance of the sensor.

With the development of science and technology, various materials have been developed for modifying electrodes. The modified sensor for nitrite detection not only increases the electrochemical reaction of  $\text{NO}_2^-$  redox but also plays a great role in expanding the detection range of nitrite and reducing the detection limit [21]. In recent years, nanomaterial sensors have become a powerful analytical tool due to the development and use of various functional nanomaterials [4]. At present, the nanomaterials commonly used to modify electrodes include graphene (GR), carbon nanotubes (CNTs), carbon nanofibers, carbon nanodots, and other carbon materials; metals, metal oxides, and other metal materials; metal-organic framework compounds [22]; conducting polymers [23]; and enzymes [24]. Carbon materials have become the most widely used materials among the above-mentioned nanomaterials due to their large specific surface area and wide range of raw materials. The metal-organic framework is a material that emerged in the later period and has attracted extensive research because of its unique and fascinating structure. Modified electrodes exhibit higher reactivity and faster electron transfer rates for nitrite detection. Although there are many electrodes modified by precious metals in metal oxides, they show good electrocatalytic properties when used for nitrate detection. For example, Salagare et al. doped palladium oxide (PdO) with RGO using an in situ chemical solution technique for nitrite sensing. The peak oxidation current of nitrite showed a linear relationship with its concentration ranging from 10 to 1500  $\mu\text{M}$ , and the LOD was 10.14  $\mu\text{M}$  [25]. Salagare et al. prepared silver nanoparticle-modified zinc oxide nanocomposites by ethylene glycol reduction method for nitrite sensing. The detection range of nitrite was 30–1400  $\mu\text{M}$ , and the detection limit was 14  $\mu\text{M}$  [26]. The application of electrodes modified by precious metals is limited in practical work due to the scarcity of precious metals and the difficulty of polymerization.

Therefore, this article does not take precious metal materials as the object of study.

This article reviews the application of nanomaterial-modified electrochemical sensors in nitrite detection in the past decade (2023–2013). Research on nitrate sensors is on the rise overall, and composites tend to outperform single materials. In addition, when summarizing the various detection limits and linear ranges for nitrite, it was found that the sensor has a wide linear range and the detection limits have been down to the micromolar level. In research, nitrite sensors have been used to detect a variety of actual samples, including water, soil, beverages, sausages, and pickles. The purpose of this article is to provide the reader with a systematic understanding of the current state of research on sensors modified with non-precious materials so that more convenient and feasible sensors can be developed.

## Nitrite sensor based on carbon

In the electrochemical method, it is not efficient when used directly to detect nitrite due to the high oxidation potential of the bare electrode. Therefore, some functional nanomaterials are commonly used to modify the electrode. Among the functional nanomaterials developed, carbon materials have attracted extensive research because of their large specific surface area and high electrical conductivity [27]. In recent years, researchers have developed a variety of electrochemical sensors modified with carbon materials of different properties. The sensors can be used for the detection of nitrite. These carbon materials include carbon nanotubes [28], graphene [29], and nanoporous carbon (NC) [30]. In this section, the application of carbon nanotubes and graphene materials in electrochemistry is mainly introduced. The properties of these nanocomposites are then summarized in Table 1.

### Nitrite sensor based on carbon nanotubes

Since CNTs have been studied, scholars have continuously used them for modifying electrochemical sensors. Carbon nanotubes are rolling graphene sheets with axis symmetry. Based on the different layers of graphene, it can be divided into single-walled nanotubes (SWCNTs) and multi-walled nanotubes (MWCNTs) [87]. Single-walled nanotubes have attracted extensive research because they can be compatible with other substances. For example, Xian et al. applied a covalent modification approach to immobilize single-walled carbon nanotubes with single-stranded deoxyribonucleic acid composites on the surface of glassy carbon electrodes (GCEs) [31]. The modified electrodes not only have a large specific surface area and good electrical conductivity, but the presence of single-walled nanotubes can

**Table 1** Electrochemical nitrite sensor based on carbon material

Electrode material	Method	Linear range (μM)	LOD (μM)	Sample	Ref.
SWCNTs/ssDNA/GCE	DPV	0.6–540	0.15	Sausage	[31]
DNA-CNTs/Cu <sup>2+</sup> /GCE	Amp	0.03–2600	0.03	–	[32]
Poly(1,8-DAN)/f-MWCNT/CPE <sup>a</sup>	Amp	0.3–6.5	0.075	Water	[33]
GC/PEDOT <sup>b</sup> /CNT/Fe <sub>3</sub> O <sub>4</sub> /GCE	DPV	0.5–150	0.022	Water	[34]
MWCNTs/PPy-C <sup>c</sup> /GCE	LSV <sup>s</sup>	500–10,500	2.3	Water	[35]
Nb <sub>2</sub> C@MWCNTs-STAB/GCE	DPV	0.1–2000	0.022	Spinach and milk	[36]
CoPe <sup>d</sup> /MWCNTs/GCE	DPV	10–1,050,000	2.11	–	[37]
CoTLMethPe <sup>e</sup> /MWCNTs/GCE	DPV	0.05–1.05	0.035	Beetroot vegetable	[38]
c-MWCNT/TiN/GCE	Amp	0.006–950	0.04	Water and meat	[39]
PBA <sup>f</sup> /MWCNTs/GCE	DPV	10–400, 400–2100	0.5	Mustard and ham sausage	[29]
GC/SWCNT/3/GCE	DPV	5–200	1.08	Tap and mineral water	[40]
HOOC-MWCNT/GCE	DPV	100–700	0.565	Pond and underground water	[41]
PPy/SDS <sup>g</sup> /f-MWCNTs/GCE	DPV	3–1120	0.11	Tap water	[42]
TiO <sub>2</sub> /MWCNT/GCE	DPV	0.02–600	0.011	Dam receiving waste	[28]
Fe <sub>2</sub> O <sub>3</sub> /MWCNTs/GCE	Amp	10–1000	0.1	Tap water	[43]
Bi <sub>2</sub> Se <sub>3</sub> @MWNTs-COOH/GCE	DPV	0.01–7000	0.002	Tap and moat water	[44]
Stir bar-shaped/N-rGO/GCE	CA <sup>l</sup>	0.2–1200, 1500–7800	0.13	Ham sausage and tap water	[22]
LRGO <sup>h</sup> /PDAC <sup>i</sup> /ION-RGO	DPV	10–400	7.2	–	[45]
Ni/PDDA <sup>j</sup> /rGO/SPCE <sup>k</sup>	CV	6–20, 20–100	1.99	Sausages and pickled vegetable	[46]
N, O co-doped LIG	DPV	5–450	0.8	Tap water and pickle water	[47]
Cu-rGO/ITO	DPV	10–100	1.875	Cheese, sausage, and salami	[48]
GO/copper terephthalate/GCE	SWV	5–625	0.3	Tap, bore well, and sewage water	[49]
rGOIm/GCE	SWV	1–1000	0.28	Tap water	[50]
rGO-MOS <sub>2</sub> -PEDOT/GCE	DPV	1–1000	0.059	Water and milk	[51]
rGO/zirconium hexacyanoferrate	SWV	0.00323–0.04198	0.00139	Water and milk	[52]
rGO/ZnO/GCE	LSV	200–4000	1.18	Tap water	[53]
AGCE <sup>l</sup> /ERGO/PBCB <sup>m</sup>	CV	30–500	2.46	Tap water	[54]
Co <sub>3</sub> O <sub>4</sub> -rGO/CNTs/GCE	Amp	0.1–8000	0.016	Tap water	[55]
CuO/H-C <sub>3</sub> N <sub>4</sub> /rGO	CV	0.2–110	0.025	–	[56]
Fe <sub>3</sub> O <sub>4</sub> /GO/COOH/GCE	DPV	1–85, 90–600	0.37	Water	[57]
Polyaniline/RGO/IDE	Amp	400–183,700	0.1	Tap water	[58]
rGO/Pani/AsM <sup>n</sup> /GCE	SWV	25–7500	10.71	Ground and sewage water	[59]
ERHG <sup>o</sup> /GCE	Amp	0.2–10,000	0.054	Tap water and liquid milk	[60]
rGO-MoS <sub>2</sub> /GCE	Amp	0.2–4800	0.17	Tap water	[61]
Ni(OH) <sub>2</sub> /sr-GO/GCE	Amp	0.1–663.6	0.07	Mineral water	[62]
RGO/MnFe <sub>2</sub> O <sub>4</sub> /PANI/GCE	DPV	0.05–12,000	0.015	Water	[63]
CuOx/ERGO/GCE	Amp	0.1–100	0.072	Tap water and meat	[64]
Fe <sub>2</sub> O <sub>3</sub> /H-C <sub>3</sub> N <sub>4</sub> /rGO/GCE	DPV	0.025~3000	0.01843	–	[65]
CuO/MWCNTs/SPE	CA	4000–6500	0.039	Tap and mineral water	[66]
LaAlO <sub>3</sub> @GO/GCE	Amp	0.01–1540.5	0.0041	Drinking water and meat	[67]
Mn-rGO-GCE	DPV	0.1–5.5	0.02	Juice and tap water	[68]
PC <sub>ST</sub> <sup>p</sup> /GCE	Amp	0.1–100	0.043	Meat	[69]
PHCNs <sup>q</sup> /GCE	Amp	0.037–6950	0.01	Pickle	[70]
CoPx@P,N-RPCs <sup>r</sup> /GCE	DPV	0.01–1184	0.005	Sausage and mineral water	[30]
Si/C/Al/SiPy <sup>+</sup> Cl <sup>-</sup>	Amp	0.2–280	0.01	Meat and water	[71]
CoOx/C/GCE	DPV	0.2–2500	0.05	Sausage	[72]
CC	Amp	0.25–3838.5	0.03	Sausage and mineral water	[73]
PANI@GO/GCE	Amp	2–44,000	0.5	Rain and tap water	[74]
(NiCo-RGO)GCE	DPV	60–860	1.8	Water cucumber juice and milk	[75]
GC/poly-TBO-SWCNT	Amp	1–4000	0.37	Wastewater	[76]

**Table 1** (continued)

Electrode material	Method	Linear range ( $\mu\text{M}$ )	LOD ( $\mu\text{M}$ )	Sample	Ref.
[PDDA/ $\alpha_2$ -K <sub>7</sub> P <sub>2</sub> VW <sub>17</sub> O <sub>62</sub> ·18H <sub>2</sub> O-CNTs] <sub>10</sub> /ITO	CV	0.05–2130	0.0367	Apple, orange, and peach juice, coconut juice, sterilized milk, sausage, and pickled vegetable	[77]
IL-SWCNT	Amp	1–12,000	0.1	Milk	[78]
Hb/IL/MWILE-modified electrode	CV	10–15,000	1.46	Sausage	[79]
MWCNTs/carbon ceramic electrode (CCE)	DPV	15–220	4.74	Spinach	[80]
GR-MWCNTs/FeNPs nanocomposite	Amp	0.1–1680	0.076	River, tap, and rain water	[81]
PDDA-rGO/GCE	Amp	0.5–2000	0.2	Drinking water	[82]
Chitosan/phenylamine-GO/GCE	Amp	5–4650	2	Tap water	[83]
CoNi NPs/ERGO/GCE	Amp	0.1–30, 30–330	0.05	Hot dog sausage, mortadella salami, and feta white cheese	[84]
Cu-NDs/RGO/GCE	Amp	1.25–13,000	0.4	River water	[85]
CTAB-GO/MWNT/GCE	DPV	5–800	1.5	Human urine	[86]

<sup>a</sup>Carbon paste electrode

<sup>b</sup>Poly(3,4-ethylene dioxy-thiophene)

<sup>c</sup>Polypyrrole-carbon black

<sup>d</sup>Cobalt (II) phthalocyanine

<sup>e</sup>Tetra L-methionine cobalt (II) phthalocyanine

<sup>f</sup>Prussian blue analogues

<sup>g</sup>Sodium dodecyl sulfate

<sup>h</sup>Light-scribed reduced graphene oxide

<sup>i</sup>Poly(diallyl dimethyl ammonium) hydrochloride

<sup>j</sup>Poly(diallyldimethylammonium chloride)

<sup>k</sup>Screen-printed carbon electrode

<sup>l</sup>Activated glassy carbon electrode

<sup>m</sup>Poly(brilliant cresyl blue)

<sup>n</sup>Polyaniline–arsenomolybdate

<sup>o</sup>Electrochemically reduced holey graphene

<sup>p</sup>Porous carbon derived from sodium tartrate

<sup>q</sup>Porous hollow carbon nanospheres

<sup>r</sup>Phosphorus/nitrogen co-doped reticular porous carbon frameworks

<sup>s</sup>Linear sweep voltammetry

<sup>t</sup>Chronoamperometry

enhance the electron transfer rate so that the sensor has high catalytic performance. Under the optimal experimental conditions, the linear range of the sensor can be gained from 0.6 to 540  $\mu\text{M}$ , and the minimum detection limit is as low as 0.15  $\mu\text{M}$  by differential pulse voltammetry (DPV). In addition, the sensor has good stability and strong anti-interference ability. The good stability of the sensor is mainly attributed to the fact that the nanocomposites are immobilized on the electrode surface by covalent bonds rather than simply physically adsorbed on the electrode surface. Based on this research, the composite material was further optimized. For example, Yang et al. used a one-step electrodeposition method to immobilize DNA-CNTs/Cu<sup>2+</sup> on the surface of a glassy carbon electrode [32]. Through cyclic voltammetry (CV), it can be found

that adding CNTs/Cu<sup>2+</sup> can enhance charge transfer and reduce the hindrance of DNA film to charge. After optimization of the experimental conditions, the sensor was measured using amperometry (Amp). The results showed that the DNA-CNTs/Cu<sup>2+</sup>-modified sensor had a linear range of  $3 \times 10^{-8}$ – $2.6 \times 10^{-3}$  M and a detection limit of  $3 \times 10^{-8}$  M (S/N = 3). The reproducibility of the sensor was studied using five identically modified electrodes, and the RSD was measured to be 4.4%. These results indicated that the reproducibility of the sensor was good. In addition, the current response of nitrite was measured every day. It was found that the current response value was maintained at more than 88% of the initial reaction after 30 days. This result indicated that the sensor had strong stability and could be detected in real samples.

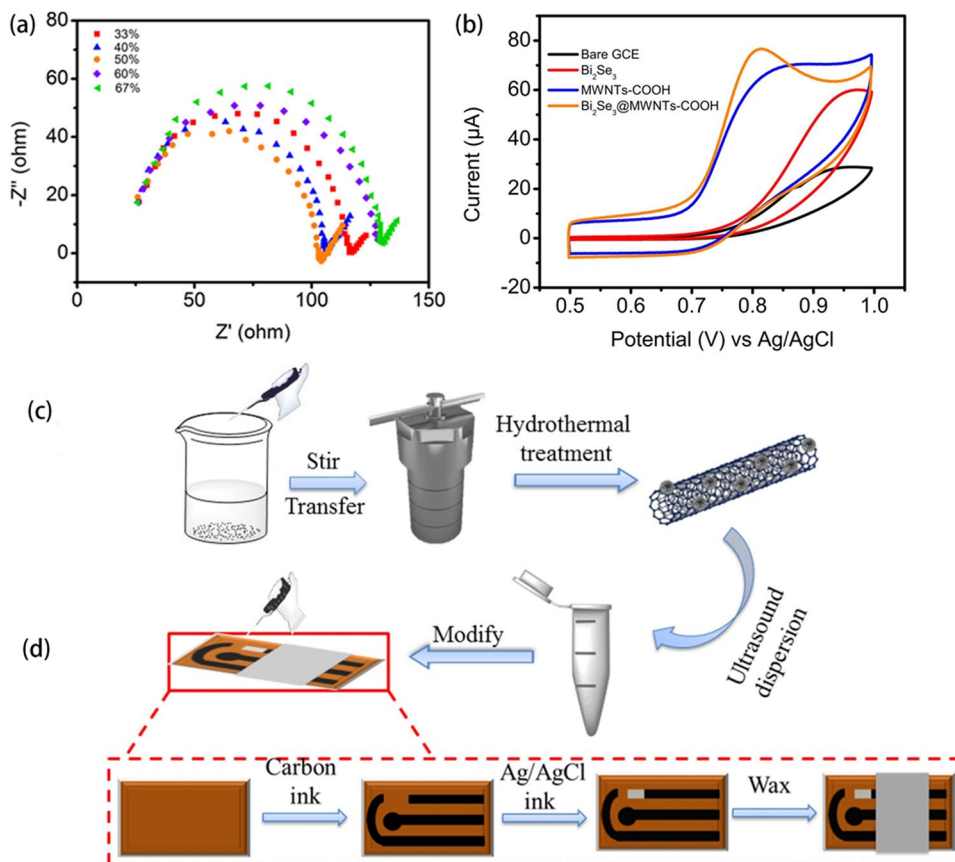
Compared with other materials, multi-walled carbon nanotubes have remarkable electrocatalytic activity and a strong current response. However, there is almost no interaction of available ions to detect a particular analyte at low concentrations, and multi-walled nanotubes are less hydrophobic in aqueous solutions. To overcome these problems, multi-walled nanotubes can be modified by adding appropriate functional groups to improve the hydrophobicity and electrocatalytic stability of the nanotubes [21, 88, 89]. For example, Sudha et al. constructed COOH-functionalized multi-walled nanotubes for modifying glassy carbon electrodes [41]. COOH-functionalized multi-walled nanotubes had more graphitic properties than the original MWCNT, so more active sites (C=C and COOH groups of HOOC-MWCNT) can interact with the analyte. The feature can achieve the purpose of low-concentration sensing. In addition, the detection range of the sensor was determined to be 100  $\mu\text{M}$ –0.7 mM, and the detection limit was 565 nM by differential pulse voltammetry. To demonstrate the practicability of the sensor, the samples of ground pond water were tested. The results showed a recovery of 102% for nitrite. To further improve the performance of this composite, it can be compounded with a metal material. For example, Zhu et al. compounded COOH-functionalized multi-walled nanotubes with  $\text{Bi}_2\text{Se}_3$  [44].  $\text{Bi}_2\text{Se}_3$ @MWNTs-COOH

nanocomposites were synthesized to modify GCE/carbon electrodes (CE) by a one-step hydrothermal method. Five samples were prepared by adding different concentrations of reagents. Among them,  $\text{Bi}_2\text{Se}_3$ @MWNTs-COOH-50% had the lowest charge transfer resistance. The result indicated that the composite has the highest electron transfer rate. By measuring the CV curves of different electrodes, it can be obtained that  $\text{Bi}_2\text{Se}_3$ @MWNTs-COOH had the largest current response value (Fig. 1). The result indicated that  $\text{Bi}_2\text{Se}_3$ @MWNTs-COOH has a larger surface area, which is favorable for nitrite adsorption. The disposable electrochemical sensor has a detection range of 0.01  $\mu\text{M}$ –7.0 mM, and the minimum detection limit is 0.002  $\mu\text{M}$  for the detection of nitrite. In short, the sensor has great potential for the detection of nitrite.

### Nitrite sensor based on graphene

Graphene is a two-dimensional carbon nanomaterial composed of  $\text{sp}^2$  hybrid orbital carbon atoms. Its structure is a honeycomb hexagonal lattice network and can be extended indefinitely [90]. Graphene has become the most promising material for nitrite detection because of its cheap raw material and good electrical conductivity [60, 91]. Graphene can be divided into graphene oxide (GO) and reduced graphene

**Fig. 1** **a** EIS of  $\text{Bi}_2\text{Se}_3$ @MWNTs-COOH-x electrodes. **b** CV curves of the different electrodes to detect 1.0-mM nitrite in 0.1-M PBS (pH 7.0) at 100  $\text{mV s}^{-1}$ . **c** Schematic diagram of the synthesis method of  $\text{Bi}_2\text{Se}_3$ @MWCNTs-COOH/CEs and the preparation process **d** [44]. Copyright 2021, Elsevier



oxide (rGO). Reduced graphene oxide includes chemically reduced graphene oxide (CrGO) and electrochemically reduced graphene oxide (ErGO). rGO has higher electrical conductivity compared to GO. So rGO is more widely used than graphene [6, 21]. However, pure graphene has serious aggregation and homogeneity problems. So electrochemical properties are usually reduced [92].

Doping graphene with various heteroatoms is an effective method to improve the structural and electrochemical properties of graphene. Yuan et al. used a simple laser engraving method to prepare N and O co-doped porous graphene under UV irradiation (Fig. 2) [47]. LIG was detected by DPV. The results showed a good linear relationship between the peak current and the analyte concentration. And the sensor had a detection range of 5~450  $\mu\text{M}$ , and the minimum detection limit was 0.8  $\mu\text{M}$ , which was 55 times lower than the detection limit of 3 mg/L set by the World Health Organization. Surprisingly, the electrode had good reproducibility and strong anti-interference ability. In short, the sensor has broad application prospects in detecting nitrite. Cheng et al. prepared graphene-based nanocomposites sb-ZnO (stir bar-shaped ZnO)/N-rGO for modifying glassy carbon electrodes by combining a novel stir bar-shaped ZnO with N-doped reduced graphene oxide using a hydrothermal method [22]. There is a large active surface area due to extra valence bonds between  $\pi$ -electron and lone pairs of N atoms in graphene oxide. The large active surface can accelerate the electron transfer rate. In addition, ZnO enhances the electron transfer capability and provides a large surface area due to a wide direct band gap and extended excitation binding

energy. With the synergistic effect of N-rGO and sb-ZnO, the nanocomposite-modified electrode has a low detection limit of 0.13  $\mu\text{M}$  and a linear range of 0.2  $\mu\text{M}$ ~1.2 mM and 1.5~7.8 mM. In addition, the recovery rate of nitrite by this sensor is between 96.0 and 103.0% in practical applications of ham sausage, sauerkraut, and tap water.

Another way to improve the sensitivity is to incorporate various nanomaterials, such as metal oxides and conducting polymers. In recent years, transition metal hydroxides have been confirmed to have high electrocatalytic activity and are promising for various applications in electrochemical sensors. For example, Salagare et al. successfully prepared cobalt-nickel-reduced graphene oxide nanoparticles by complexing transition metal mixed oxides  $\text{NiCo}_2\text{O}_4$  with RGO using urea nitrate complexing agent auto-ignition method [75]. The nanocomposite has a unique porous structure and layered connections. CV and DPV method was used to study the electrocatalytic behavior of the material towards nitrite. The results showed that the composite-modified graphite electrode (NiCo-RGO) had a larger peak anodic current than the bare graphite electrode. The linear range was found to be 60~860  $\mu\text{M}$  with a detection limit of 18.0  $\mu\text{M}$  about the NiCo-RGO/GCE-based sensor for nitrite detection by the DPV method. In addition, the material showed good reproducibility, repeatability, and stability for electrochemical sensing of nitrite. Good recoveries were obtained in real samples of water, cucumber juice, and milk. The sensor has good prospects for commercialization. Yılmaz-Alhan et al. prepared a two-dimensional carbon-metal oxide composite electrode to modify the glassy carbon electrode

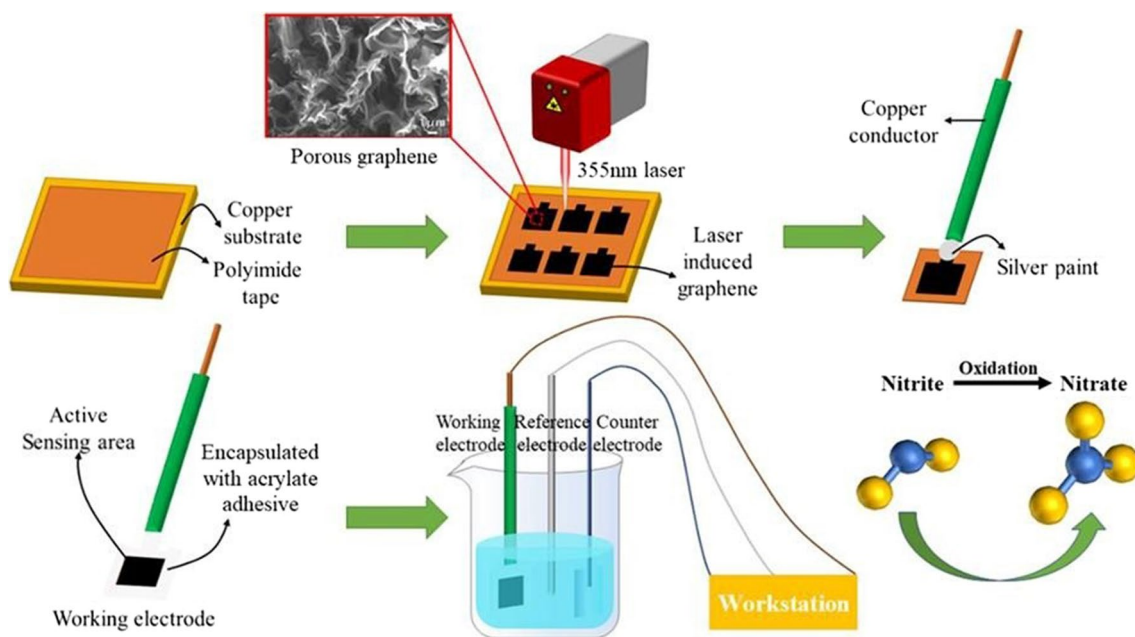


Fig. 2 Fabrication scheme of LIG and electrochemical sensing electrodes [47]. Copyright 2022, Elsevier

[68]. Transition metal manganese oxide was doped with reduced graphene oxide and then combined with a glassy carbon electrode to form  $\text{MnO}_2\text{-rGO/GC}$  electrode. The  $\text{MnO}_2\text{-rGO}$ -based composites have good electrochemical properties due to the high electrical conductivity of the  $\text{MnO}_2\text{-rGO/GC}$  electrode, which enables rapid electron transfer between the redox couple and the electrode surface. The sensor has a detection limit as low as  $0.02 \mu\text{M}$  and a detection range of  $0.1\text{--}5.5 \mu\text{M}$ . The  $\text{MnO}_2$ -reduced graphene oxide composite was used to test fruit juice and tap water with good recovery and high interference resistance. Wang et al. prepared nanocomposites ( $\text{Ni(OH)}_2\text{/sr-GO}$ ) of nickel hydroxide and reduced graphene oxide by a one-step solvothermal method without reducing agents and bases. They constructed an electrochemical sensor for nitrite detection [62]. In electrochemical tests, the  $\text{Ni(OH)}_2\text{/sr-GO}$  nanocomposites showed high electrocatalytic activity. The detection range of the sensor is  $0.1\text{--}663.6 \text{ mM}$ , and the detection limit is  $0.07 \text{ mM}$  ( $S/N = 3$ ) by amperometry. In addition, the sensor has good selectivity and stability, and low relative deviation with good recovery can be obtained to detect nitrite in water samples. Cheng et al. prepared perovskite oxides  $\text{La}_{0.8}\text{Sr}_{0.2}\text{MnO}_3$  (LSM) and reduced graphene oxide by sol-gel method and Hummer method [93]. Then, the  $\text{LSM/rGO}_x$  composites were successfully prepared by mixing the two in different proportions by probe ultrasound. At  $15 \text{ wt\%}$  rGO content, LSM particles have the best dispersion on rGO. In addition to this, composites have the largest peak current and the smallest transfer resistance in CV and electrochemical impedance tests. This shows that  $\text{LSM/rGO}_{1.5}$  composites have the strongest oxidation ability to nitrite and the fastest electron transfer rate. The catalytic mechanism of  $\text{LSM/rGO}_x$  for nitrite oxidation can be inferred from electrochemical tests. Firstly,  $\text{Mn(II)}$  or  $\text{Mn(III)}$  is electrochemically oxidized to  $\text{Mn(III)}$  and  $\text{Mn(IV)}$ , and secondly,  $\text{Mn(III)}$  and  $\text{Mn(IV)}$  chemically oxidize  $\text{NO}_2^-$  to  $\text{NO}_3^-$  (Fig. 3). The three-electrode sensor based on  $\text{LSM/rGO}_x$  has an ultra-low detection limit ( $0.016 \mu\text{M}$ ), good stability, and accuracy for  $\text{NO}_2^-$  detection in water. And it is expected to be used for the detection of nitrite in real environments. Among the conductive polymers, polyaniline has been widely studied for its good conductivity and stability. For example, Sivakumar et al. prepared polyaniline-@graphene oxide ( $\text{PANI@GO}$ ) nanocomposites and used them to modify GCE [74]. The electrochemical performance of  $\text{PANI@GO/GCE}$  for nitrite oxidation was evaluated by comparing  $\text{PANI@GO/GCE}$  with  $\text{GO/GCE}$ ,  $\text{PANI/GCE}$ , and bare GCE electrodes by CV technique. The results showed that the electrode had the highest oxidation current (about  $45.7 \mu\text{A}$ ) and the lowest overpotential ( $0.83 \text{ V}$ ). The electrode had a wide linear range ( $2\text{--}44,000 \mu\text{M}$ ), high sensitivity ( $117.23 \mu\text{A mM}^{-1} \text{ cm}^{-2}$ ), and low detection limit ( $0.5 \mu\text{M}$ ). In addition,  $\text{PANI@GO/GCE}$  electrode had good selectivity, stability, repeatability,

and reproducibility in nitrite detection. A good recovery rate ( $98.07\text{--}106.11\%$ ) was obtained when the electrode was used in real-time applications of rain water and tap water samples, indicating that the sensor is suitable for real-time applications. Li et al. successfully prepared polyaniline/reduced graphene oxide composites by combining polyaniline with reduced graphene oxide by in situ electrochemical reduction and cyclic voltammetry electrochemical polymerization, which was used to modify the interdigital electrode (IDE) [58]. The electrochemical test on the composite showed that the  $\pi\text{-}\pi$  superposition force between aniline and rGO made electron transfer easier and contributed to the conductivity of IDE compared to bare electrodes. At the same time, the increase in conductivity and the transfer of electrons are conducive to the polymerization of aniline, which can increase the current and reduce the oxidation potential. The property gives the sensor good electrochemical performance. The detection range of the sensor is  $0.4\text{--}183.7 \text{ mM}$ , and the detection limit is  $0.1 \mu\text{M}$ . Reduced graphene oxide is a derivative of graphene, different graphene materials can be obtained depending on the reduction method. Among them, ErGO is widely used because of its easy control and safety in synthesis. For example, Yue et al. prepared  $\text{CuO}_x\text{/ErGO}$  nanohybrids by electrodeposition method [64]. Depending on the pH,  $\text{CuO}_x\text{/ErGO}$  nanohybrids with different morphologies can be synthesized. With the gradual increase of pH,  $\text{CuO}_x\text{/ErGO}$  can take on peony-shaped, honeycomb-shaped, rose-shaped, and purple myrtle-shaped. Among them, the electrochemical sensor prepared from honeycomb  $\text{CuO}_x\text{/ErGO}$  showed the highest electrocatalytic activity for nitrite oxidation. The sensor has a detection limit as low as  $0.072 \text{ mM}$  and a detection range of  $0.1\text{--}100 \text{ mM}$ . In addition, the recovery rate of the sensor was between  $94.29$  and  $106.21\%$  when detecting drinking water. The method is highly accurate in detecting nitrite and has good prospects for development and application.

## Nitrite sensor based on metal-organic frameworks

Among functional nanomaterials, metal-organic frameworks are the later emerging porous materials. Metal-organic frameworks are important porous crystalline coordination polymers that are self-assembled by various metal ions or metal clusters and organic ligands through coordination bonds. It has the advantages of a large specific surface area, high porosity, and adjustable pore size [94–96]. At present, it has been widely used in electrochemical sensing (Fig. 4) [97]. However, the original MOF is chemically less stable because of weak coordination bonds and active groups in the MOF [98]. In addition to this, the original MOF conductivity is lower. This is due to less skeletal overlap between the

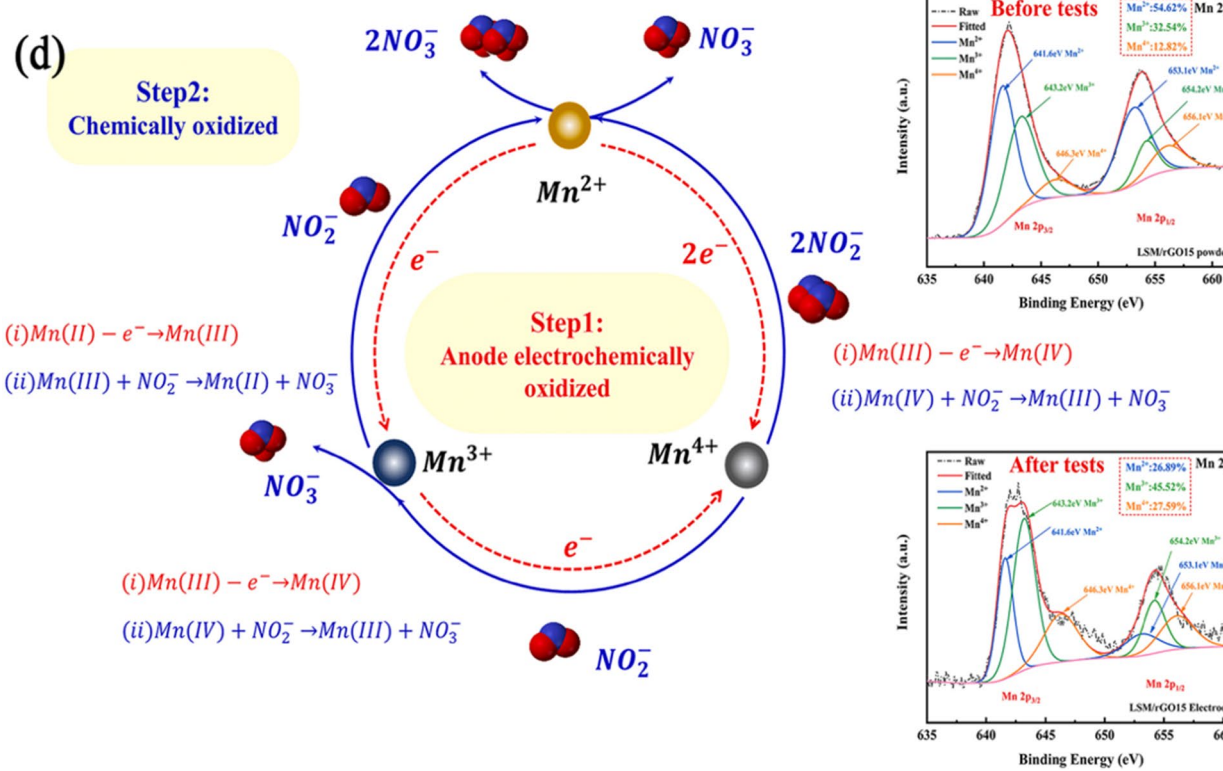
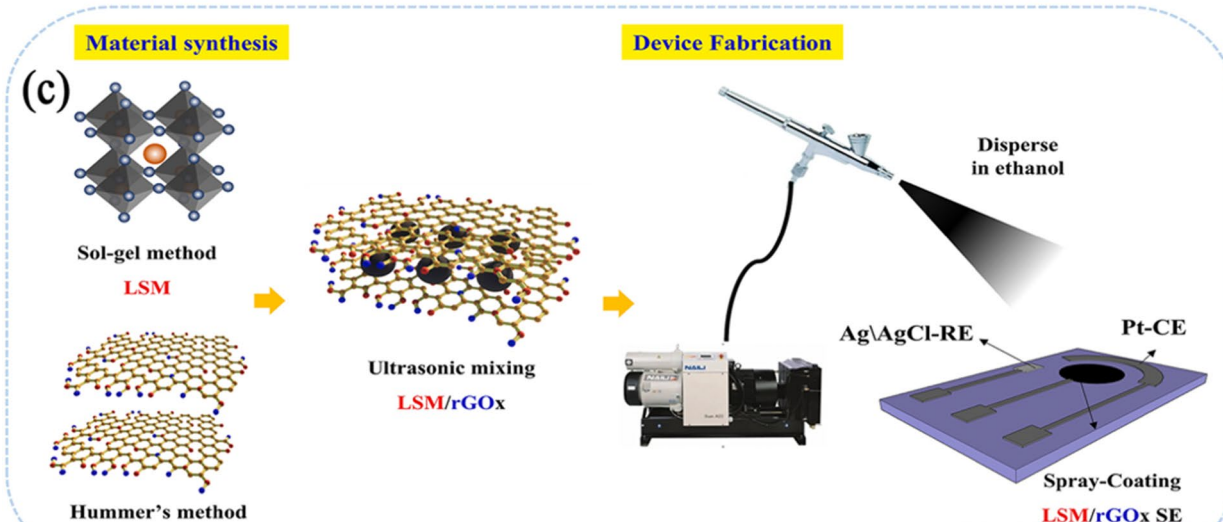
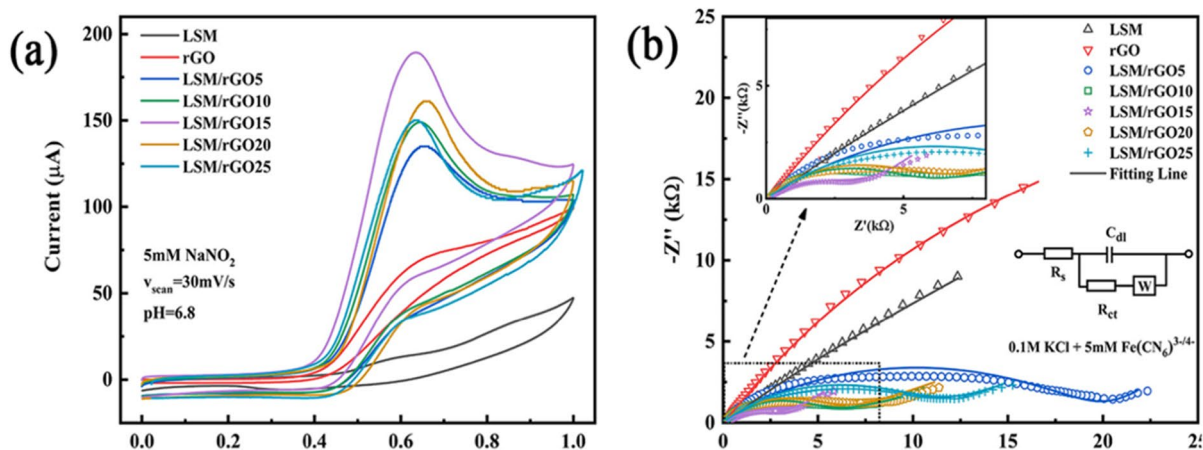




**Fig. 3** **a** CV curve of the sensor at a scanning rate of  $30 \text{ mV s}^{-1}$  in  $5\text{-mM NaNO}_2$ . **b** Nyquist diagram of the sensor in  $0.1\text{-M KCl}$  solution containing  $5\text{-mM } [\text{Fe}(\text{CN})_6]^{3-/4-}$ . **c** Description of making electrochemical sensor based on LSM/rGO<sub>x</sub> sensor electrode. **d** Schematic diagram of nitrite oxidation reaction mechanism and XPS results of Mn before and after electrochemistry tests [93]. Copyright 2022, Elsevier

p-orbital of the ligand and the d-orbital of the metal ions. Performance is not ideal when used for inspection [99]. In order to overcome these disadvantages, they are generally modified. One approach is to combine metal-organic frameworks with other functional materials to form composites, and the other is to pyrolyze MOFs to obtain their derivatives [100]. This section mainly introduces the application of MOF composites and their derivatives in electrochemical sensors. The performance of MOFs in electrochemical sensors is shown in Table 2.

### Nitrite sensor based on MOF composite

In MOF-based composites, electroactive materials are often used to prepare continuous composites. These materials include metal oxides, carbon-based materials, and conductive polymers. Carbonaceous materials such as graphene, carbon nanofibers, and graphite dots are the preferred substrate materials for the preparation of composite materials. Among many kinds of MOFs, Cu-MOF materials have good electrocatalytic performance due to the REDOX properties of  $\text{Cu}^+/\text{Cu}^{2+}$ . For example, Sivakumar et al. prepared copper nanoporous carbon (Cu@NPC) nanoporous structures using a solvothermal method based on a two-step method (Fig. 5d) [119]. However, its poor electrical conductivity has limited the further development of electrochemical sensing. Adding carbon material to Cu-MOF material can overcome this problem. Due to the characteristics of  $\pi$ - $\pi$  interaction and hydrogen bond interaction between carbon-based materials and MOFs, the conductivity and electron transfer rate can be accelerated in MOFs. For example, copper-functionalized MOF materials were synthesized by compounding copper ions with UiO-67-BPY and subsequently combined copper-chelated UiO-67-BPY MOF with graphene oxide for modification of electrodes [104]. In electrochemical tests, the current of Cu@MOF/ERG (electrochemically reduced graphene)/GCE is large compared to Cu@MOF/GCE, indicating faster electron transfer. The possible reason is that the  $\pi$ -electron conjugation effect of MOFs is amplified due to the chelation of bipyridyl ligands with copper, thereby enhancing the charge conductivity. In addition, the synergistic effect between ERG and MOFs makes the electrode surface more stable, which is beneficial to increase the specific surface area of the electrode and improve its sensitivity in electrochemical detection. The sensor was investigated through the DPV, and its detection range was  $10\text{--}6000 \mu\text{M}$

with the detection limit of  $1.2 \mu\text{M}$  for nitrite. In addition, the electrode had excellent reproducibility and stability and had great potential for future sensor platforms. Ambaye et al. synthesized carbon black (CB)/Cu-MOF nanocomposites via ultrasound and used them to modify SPCE (Fig. 5c) [117]. CB/Cu-MOF/SPCE electrodes were compared with SPCE, Cu-MOF/SPCE, and CB/SPCE electrodes by CV method and LSV in order to study the electrochemical response of electrodes to nitrite detection. The results showed that the CB/Cu-MOF/SPCE electrode had the highest current response and was 5 times higher than that of bare SPCE (Fig. 5a, b). The electrode material had a wide detection range ( $1.0\text{--}200.0 \mu\text{M}$ ) and low detection limit ( $0.084 \mu\text{M}$ ) when used for nitrite sensing. The electrochemical sensing of nitrite showed good reproducibility, repeatability, and stability. In addition, CB/Cu-MOF/SPCE obtained a satisfactory recovery rate ( $100.90\text{--}103.40\%$ ) in the detection of nitrite in wastewater samples. The results showed that the sensor has great potential in the detection of nitrite in aquatic substrates. Salagare et al. successfully synthesized a composite material based on carboxyl-functionalized MWCNTs/Co-MOFs by solvothermal method and successfully built a sensor for nitrite determination [118]. Under optimal experimental conditions, the sensor based on this composite exhibits excellent electrocatalytic performance. It has a wide linear range ( $80\text{--}1160 \mu\text{M}$ ) and a low detection limit ( $18.8 \mu\text{M}$ ). In addition, the sensor obtained satisfactory recoveries for the determination of nitrite in beverage and water samples, which is promising for application.

In the construction of heterostructures, the hybridization of MOFs and iron-based oxides is more widely used. Compounding MOFs with iron oxides can significantly improve the electrical conductivity and catalytic activity of the materials. For example, Amali et al. constructed an electrochemical sensor platform for nitrite detection using  $\text{Fe}_2\text{O}_3$  NPs/Cu-BDC (copper(II)-benzene-1,4-dicarboxylate) MOF-modified screen-printed carbon electrode [103]. The composites were characterized, and the results proved to be successfully synthesized. The Rct of the material was significantly reduced due to the addition of  $\text{Fe}_2\text{O}_3$  NPs. The reason is that the synergistic effect of both reduces the interface electron transfer resistance of the composite, which is conducive to improving the electrocatalytic activity of nitrite oxidation. Under the best experimental conditions, the electrode was studied using amperometry, and the results demonstrated that the sensor has a wide detection range and low detection limit, the detection range is  $1\text{--}2000 \mu\text{M}$ , and the detection limit is  $0.074 \mu\text{M}$  ( $S/N = 3$ ). Among the conductive polymers, polypyrrole is widely used because of its good electrical conductivity, ease of polymerization, and low cost [120, 121]. In recent years, conductive polypyrrole and metal-organic skeleton composites have made great progress in the field of electrochemistry. For example, Xu et al.

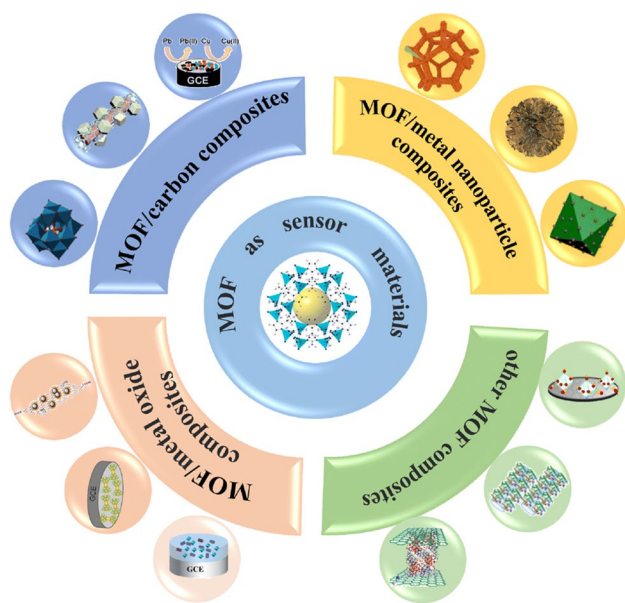


**Fig. 4** Application of MOF composites in electrochemical sensors [97]. Copyright 2023, RSC Advances

successfully prepared a new PPy/UiO-66 nanocomposite by compounding PPy with UiO-66 by in situ polymerization [122]. In the electrochemical test, the sensors prepared

from PPy/UiO-66 composite not only increased the activity of catalytic nitrite but also increased the conductivity. The enhanced performance of the sensor may be due to the good electrical conductivity of the conductive polypyrrole that promotes electron transfer in the nanocomposite and provides a large specific surface area for the adsorption and reaction of  $\text{NO}_2^-$ . The large surface area facilitates the catalytic oxidation of analytes. The sensor based on PPy/UiO-6 composite has a detection range of 0.05–1055.5  $\mu\text{M}$  and a detection limit of 0.037  $\mu\text{M}$ . It can be used as a potential nitrite sensing material.

### Nitrite sensor based on MOF derivatives

The preparation of MOF derivatives can not only retain the structural properties of parent MOFs but also enhance the electrical conductivity and catalytic activity of the parent body. There is great potential for electrochemical analysis [88]. In recent years, two-dimensional (2D) ZIF derivatives have attracted much attention due to their low diffusion resistance and easily available active centers and have been successfully applied to energy storage and antibiotic removal. Yang et al. first synthesized Co-ZIF-L in rod form and then carbonized it under an Ar atmosphere to obtain CoN-CRs (Fig. 6g) [109]. CoN-CSs were obtained by pyrolysis of the flakes of Co-ZIF-L. The prepared materials were

**Table 2** MOF-based electrochemical nitrite sensor

Electrode material	Method	Linear range ( $\mu\text{M}$ )	LOD ( $\mu\text{M}$ )	Sample	Ref.
MIL-53(Fe)/GCE	Amp	0.4–7000	0.36	Disinfection and tap water	[101]
Zn-TCPP(BP)/FTO <sup>u</sup>	Amp	1–2000	0.26	Tap and lake water	[102]
$\text{Fe}_2\text{O}_3$ NPs/Cu-BDC <sup>v</sup> MOF/SPCE	Amp	1–2000	0.074	Tap and mineral water	[103]
Cu@MOF/ERG/GCE	DPV	10–6000	1.2	Tap and river water	[104]
Nickel phthalocyanine-MOF	DPV	10–11,500,000	2300	–	[105]
Cu-MOF-GO/GCE	Amp	0.1–100	0.00147	Water	[106]
MWCNTs/Zr-aminoterephthalate	SWV	2–440	0.22	Root nodule	[107]
Cu@C@ZIF-8/GCE	DPV	0.1–300	0.033	Sausage	[108]
CoN-CRs/MGCE	Amp	0.5–4000, 4000–8000	0.17	Sausage and tap water	[109]
Ni/Co, N-CP/GCE	CA	1–500	0.094	Milk and tap water	[110]
$\alpha\text{-Fe}_2\text{O}_3$ /CNT hybrids/GCE	Amp	0.5–4000	0.15	Pond and tap water	[111]
Cu-Ni-BTC-CPE	Amp	1.0–1536, 1536–3636	0.4	Waste water	[112]
ZIF-67C@rGO/NiNPs/GCE	Amp	0.2–123, 123–473	0.086	Sausage	[113]
Cu-MOF/rGO hybrid/GCE	CA	3–40,000	0.033	Pond water	[89]
CuNps/CNTs/mGCE	Amp	5–705	0.18	Tap water	[114]
C-A Zn/Co-Fe PNSs@CC	Amp	1.25–701.25	0.44	Sausage and pure water	[115]
CNFs-Bi-MOF/GCE	Amp	0.02–2000	0.000184	Water	[116]
CB/Cu-MOF/SPCE	LSV	1–200	0.084	Wastewater	[117]
$\alpha\text{-Fe}_2\text{O}_3$ -CNTs/GCE	CV	0.5–4000	0.15	Tap and pond water	[111]
Carboxyl-functionalized MWCNTs/Co-MOFs	DPV	80–1160	18.78	Water and beverage	[118]

<sup>u</sup>4,4,4,4-(Porphine-5,10,15,20-tetra)l-tetrakis(benzoic acid) fluorine-doped  $\text{SnO}_2$  transparent conductive glass (FTO)

<sup>v</sup>copper(II)-benzene-1,4-dicarboxylate (Cu-BDC)

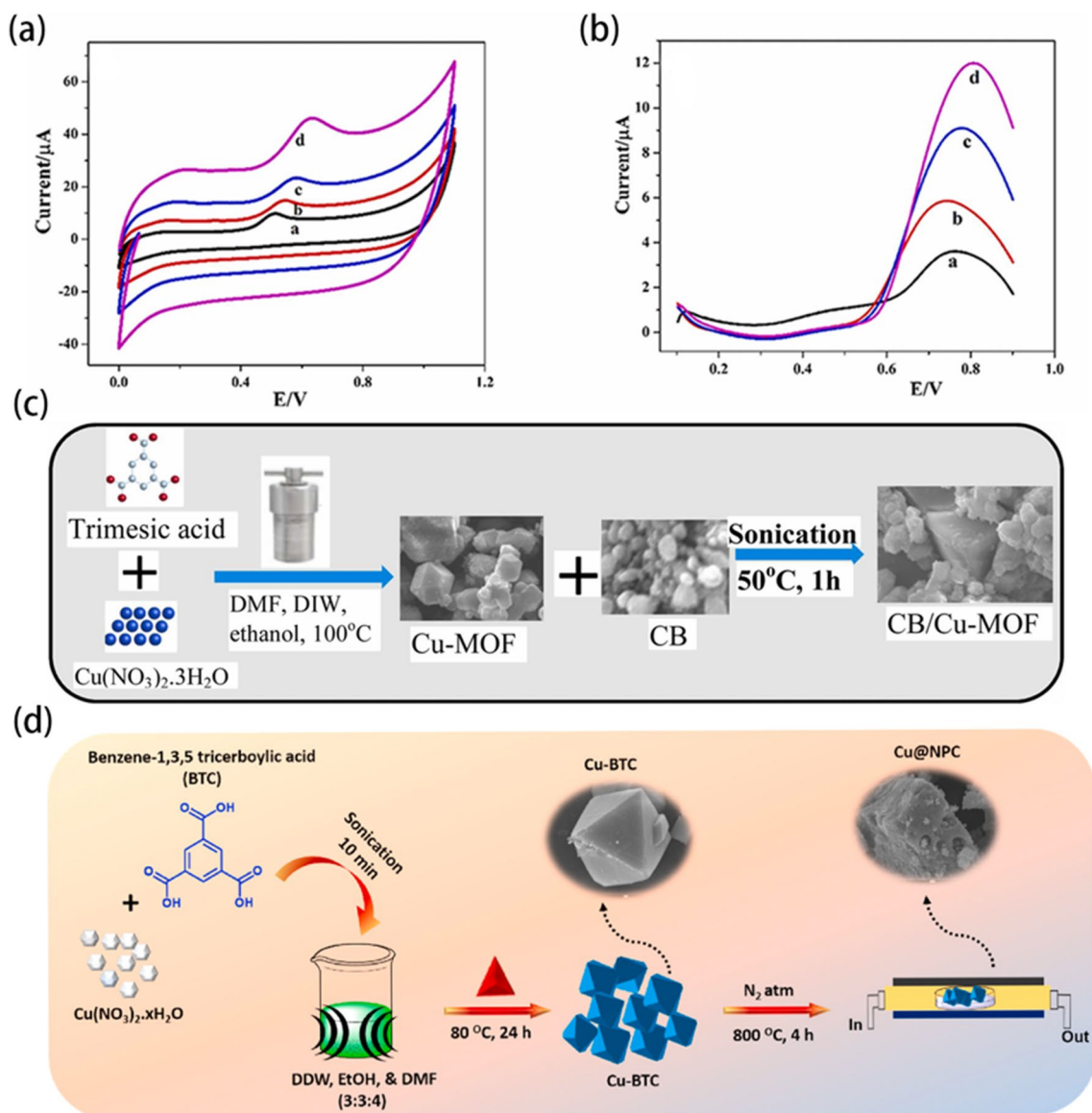


**Fig. 5** **a** CV and **b** LSV responses of 100- $\mu\text{mol L}^{-1}$  nitrite at (a) bare-SPCE, (b) Cu-MOF/SPCE, (c) CB/SPCE, and (d) CB-Cu-/SPCE. **c** Schematic description of the preparation procedures of the CB/Cu-

MOF [117]. Copyright 2023, Elsevier. **d** Schematic representation of Cu-BTC and Cu@NPC [119]. Copyright 2023, Elsevier

analyzed by a series of techniques, and the results showed that CoN-CRs had stronger nitrite detection performance than CoN-CSs. The possible reason is that CoN-CRs have better surface area and more accessible active sites. Under optimal experimental conditions, the CoN-CRs-based sensors have a wider linear range of 0.5–8000  $\mu\text{M}$  and a detection limit of 0.17  $\mu\text{M}$ . The sensor has been successfully applied to the detection of nitrite in sausage and tap water with satisfactory recoveries. In conclusion, CoN-CRs are a promising sensing material for nitrite detection. Most of the current studies have focused on two-dimensional compounds of MOFs, and fewer studies have been conducted on three-dimensional compounds. Therefore, it is of great

significance to study the MOFs of ternary composite systems. Gao et al. prepared the core-shell heterostructures of Cu@C@ZIF-8 composites by lysing Cu-MOFs@ZIF-8 under an Ar atmosphere as an electrochemical sensing platform for nitrite detection [108]. Due to the large specific surface area and high catalytic activity of the Cu@C, ZIF-8 had excellent electrocatalytic activity for nitrite detection. In the electrochemical test, the sensor has a linear response range of 0.1–300.0  $\mu\text{M}$  and a lower detection limit of 0.033  $\mu\text{M}$ . Besides, the sensor has good stability and reproducibility. In addition, the sensor's good selectivity is mainly attributed to the ZIF-8's narrow penetration channel. The sensor has been applied to the detection of nitrite in sausages

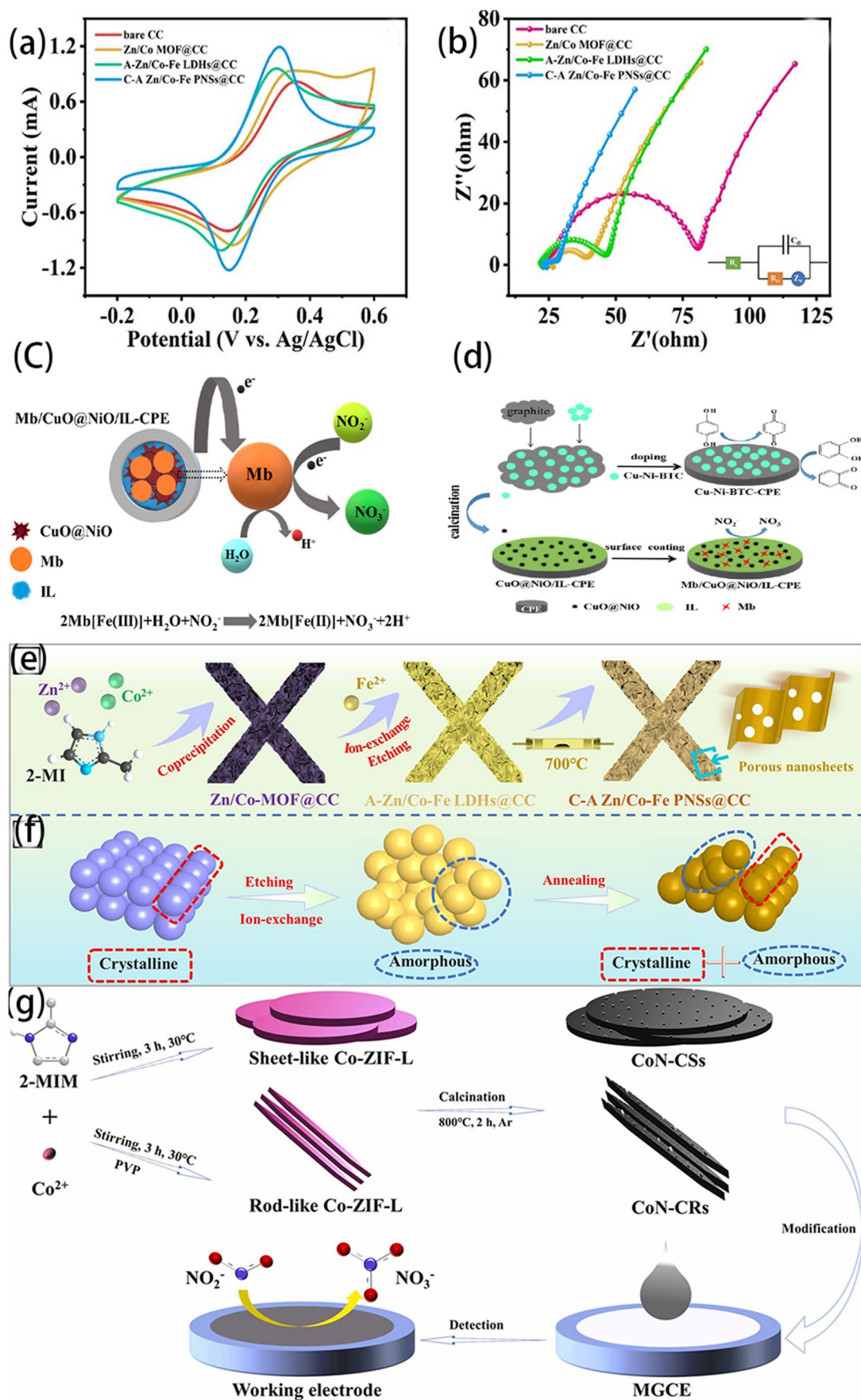


**Fig. 6** **a** CV results of 0.1-M KCl at different electrodes in 5.0-mM  $[\text{Fe}(\text{CN})_6]^{3-/4-}$  solution [115]. Copyright 2023, Elsevier. **b** EIS results at different electrodes in 5.0-mM  $[\text{Fe}(\text{CN})_6]^{3-/4-}$  solution and 0.1-M KCl [115]. **c** The mechanism of nitrite sensing [112]. Copyright 2020, Elsevier. **d** Schematic diagram of C-A Zn/Co-Fe synthesis PNSs@CC [115]. **e** Schematic diagram of synthesis mechanism [115]. **f** Schematic diagram of the synthesis method of Mb/CuO@NiO/IL-CPE and the preparation process [112]. **g** Description of the construction of CoN-CSs and CoN-CRs for nitrite detection [109]. Copyright 2022, Elsevier

with satisfactory results. In addition, Zhe et al. successfully constructed crystalline-amorphous zinc/cobalt iron porous nanosheets (C-A Zn/Co-Fe PNSs) on carbon cloth (CC) using a multi-step heterogeneous synthesis strategy [115]. By characterizing the composites, the results show that it is composed of interlaced carbon fibers and uniformly distributed hybrid nanosheet. And the special hybrid structure of the nanosheets is conducive to local enrichment of nitrite. Among the prepared materials, C-A Zn/Co-Fe PNSs@CC have the largest oxidation peak current and the lowest charge transfer resistance (Fig. 6a, b, d, e). These advantages show that C-A Zn/Co-Fe PNSs@CC has fast electron transfer ability and more significant conductivity. In addition, sensors based on C-A Zn/Co-Fe PNSs@CC have the advantages of wide linear range (1.25–4001.25  $\mu\text{M}$ ), low detection limit (0.44  $\mu\text{M}$ ), and high sensitivity (1297.13  $\mu\text{A}/(\text{mM cm}^2)$ ). This study provides a new way for the development of catalysts with excellent electrocatalytic activity and has great application prospects in nitrite detection. Dong et al. prepared Ni-MOF by microwave radiation and converted  $\text{Cu}^{2+}$  and  $\text{Ni}^{2+}$  ions into Cu/Ni organic skeletons to form Cu-Ni-BTC (1,3,5-benzenetricarboxylic acid, H3BTC) [112]. Then, the Cu-Ni-BTC is calcined to obtain a derivative CuO@NiO. Finally, myoglobin (Mb) is fixed on a sensing interface based on a CuO@NiO and ionic liquid (IL) composite membrane (Fig. 6f). Electrochemical tests showed that Mb maintained biological activity on the surface of CuO@NiO/IL composite membrane. Mb/CuO@NiO/IL has good electrocatalytic activity for nitrite. The nitrite sensing mechanism is shown in (Fig. 6c). Mb/CuO@NiO/IL-CPE (carbon paste electrode)-based sensors have linear ranges of 1.0–1536  $\mu\text{M}$  and 1536–3636  $\mu\text{M}$  for  $\text{NO}_2^-$ , with detection limits as low as 0.4  $\mu\text{M}$ .

### Nitrite sensor based on metal materials (excludes non-precious metals)

In recent years, electrochemical sensors based on different chemically modified electrodes have been manufactured. Among them, metal material is a commonly used electrode-modified material. Its surface size is adjustable, and it has good electrocatalytic activity and can be used as a sensor for

long-term stability and selectivity at relatively low temperatures [123, 124]. This section focuses on the application of non-precious metal materials as well as composite materials in nitrite sensors. The properties of such nanomaterials are summarized in Table 3.

### Nitrite sensor based on metal oxides (excludes non-precious metals)

In recent years, metal oxides prepared by suitable methods have the advantages of a larger specific area, good electrical conductivity, low price, and better stability. Due to these advantages, metal oxides are widely used in the research of nitrite sensors [8, 125]. Puspalak et al. successfully synthesized cobalt oxide nanoparticles for modification of CPE electrodes by precipitation and calcination method using green synthesis method with sugarcane juice as capping agent [154]. The CV method shows that the electrode has a certain response value for different concentrations of nitrite. In Amp detection, sensors based on this electrode have a wide detection range (50–800  $\mu\text{M}$ ) and a low detection limit (0.3  $\mu\text{M}$ ) in the detection of nitrite. What is more, the sensor can be used to detect nitrite in farmland soil samples, which can alleviate soil pollution to a certain extent and has a greater application prospect. As a kind of multi-purpose metal oxide,  $\text{TiO}_2$  has been applied in the field of electrochemical sensing because of its advantages of good biocompatibility, high conductivity, and low cost. Salagare et al. successfully prepared  $\text{TiO}_2$ -RGO nanocomposites by compositing  $\text{TiO}_2$  with RGO and used them to modify a glassy carbon electrode to construct a nitrite sensing platform [155]. The composite material has larger surface area, higher electrical conductivity, and excellent nitrite electrocatalytic activity. By CV and LSV methods, it was found that the oxidation peak of the  $\text{TiO}_2$ -RGO electrode to nitrite was higher than that of other electrodes, and the electrode based on the composite material had a high sensitivity (4.853  $\mu\text{A}/\mu\text{M cm}^2$ ), a wide linear range (10–2000  $\mu\text{M}$ ), and a low detection limit (0.006  $\mu\text{M}$ ). In addition, the sensor has obtained a good recovery rate in the determination of  $\text{NO}_2^-$  in water and buttermilk samples and has a good application prospect. Among many metal oxide-based nanomaterials, ZnO is recognized as the best nanostructure due to its wide band gap and strong binding energy [159, 160]. However, most of the ZnO-based nanomaterials prepared have the disadvantages of high detection limit and low sensitivity at present. It is well known that the topography of nanomaterials has a great influence on the performance of the sensor, and the large specific surface area can accelerate the electron transfer during the sensing process [161]. Therefore, it is possible to start by changing the morphology of ZnO. For example, Cheng et al. synthesized a unique approximately nearly spherical ZnO nanostructure by solvothermal method [127].

**Table 3** Non-precious metal-based electrochemical nitrite sensor

Electrode material	Method	Linear range ( $\mu\text{M}$ )	LOD ( $\mu\text{M}$ )	Sample	Ref.
Sn-CeO <sub>2</sub> /GCE	CA	10–600	0.016	Pond water	[125]
Carbon black/NiCo <sub>2</sub> S <sub>4</sub> @CeO <sub>2</sub> /GCE	Amp	0.2–7400	0.03	Tap and mineral water	[126]
Near-spherical ZnO/GCE	CA	0.6–220, 460–5500	0.39	Ham sausage, pickle, tap water	[127]
MnO <sub>2</sub> /PANI/GCE	CA	19.98–732.17	1.08	Water	[128]
CuO/NiO/FTO	Amp	1–1800	0.013	Tap water	[129]
MoO <sub>3</sub> /Co <sub>3</sub> O <sub>4</sub> /CC	Amp	0.3125–4514	0.075	Water and sausage	[130]
NiCo <sub>2</sub> O <sub>4</sub> /GCE	Amp	10–300	1.04	Tap water and river water	[131]
FeSeNR/CC	Amp	0.625–6775.5	0.07	Pickled vegetables	[132]
TiO <sub>2</sub> -Ti <sub>3</sub> C <sub>2</sub> TX/CTAB/CS/GCE	DPV	3–250, 250–1250	0.85	Tap and sea water and milk	[133]
NiP/NF	Amp	0.1–4000	0.01	Drinking water	[134]
APJCP-SP-FTO <sup>w</sup>	Amp	2.5–1300	0.437	Tap water	[135]
MnO <sub>2</sub>	DPV	10–800	0.5	–	[136]
a-MnO <sub>2</sub> -MoS <sub>2</sub> /GCE	Amp	100–800	16	Drinking water	[137]
MoSe <sub>2</sub> MoO <sub>3</sub> /GCE	CV	2.5–80	0.1	Potable and tap water	[138]
CuO NPs/GCE	LSV	10–50	1.1	–	[124]
Cu/CBSA NFNs <sup>x</sup> /GCE	DPV	0.5–500	0.1	Mineral water	[139]
NiFe <sub>2</sub> O <sub>4</sub> -CPE	Amp	0.1–1000	0.1236	Tap water	[140]
NiFe-LDH NSAs/CC	Amp	5–1000	0.02	Tap and Dongpu reservoir water	[141]
CFO/SPCE	Amp	0.016–1921	6.6	Tap water and mineral water	[142]
Co <sub>3</sub> O <sub>4</sub> -DCS/GCE	Amp	6.6–300, 300–13,840	0.22	Tap water and milk	[143]
CeO <sub>2</sub> -CuO/GCE	CA	10–5000	10	–	[144]
CuO/NiO/GC	Amp	1–5000	0.5	Urine	[145]
MnO <sub>2</sub> /GO-SPE	CV	0.1–1, 1–1000	0.09	Tap and packaged water	[146]
NiCo <sub>2</sub> CO <sub>3</sub> (OH) <sub>2</sub> /GCE	Amp	5–4000	0.002	–	[147]
Fe <sub>2</sub> O <sub>3</sub> @MoS <sub>2</sub> /GCE	Amp	2–6730	1	Drinking water and river water	[148]
Fe <sub>3</sub> O <sub>4</sub> /RGO/GCE	DPV	10–2882	0.1	Tap, rain, and river water	[149]
PrFeO <sub>3</sub> -MoS <sub>2</sub> /CS/GCE	Amp	5–3000	1.67	Tap water	[150]
Fe <sub>3</sub> O <sub>4</sub> /MoS <sub>2</sub> /GCE	Amp	0.5–328	0.2	–	[151]
TOSC-MoS <sub>2</sub> /GCE	Amp	6–3140, 3140–4200	2	Drinking and river water	[152]
PANI-MoS <sub>2</sub> /GCE	Amp	4.0–4834	1.5	Drinking and river water	[153]
CoO@CPE	Amp	50–800	0.3	Soil	[154]
TiO <sub>2</sub> -RGO/GE	LSV	10–2000	0.006	Tap and ground water, buttermilk	[155]
NP-Fe <sub>2</sub> O <sub>3</sub> -CoO/GCE	Amp	200–16,200	0.1	Sausage	[156]
SiO <sub>2</sub> /C/Mn(II) phthalocyanine	CV	0.79–15.74	0.2	Water and sausage meat	[157]
TiO <sub>2</sub> /carbon ionic liquid electrode	LSV	0.5–1500	0.2	Sausage	[158]

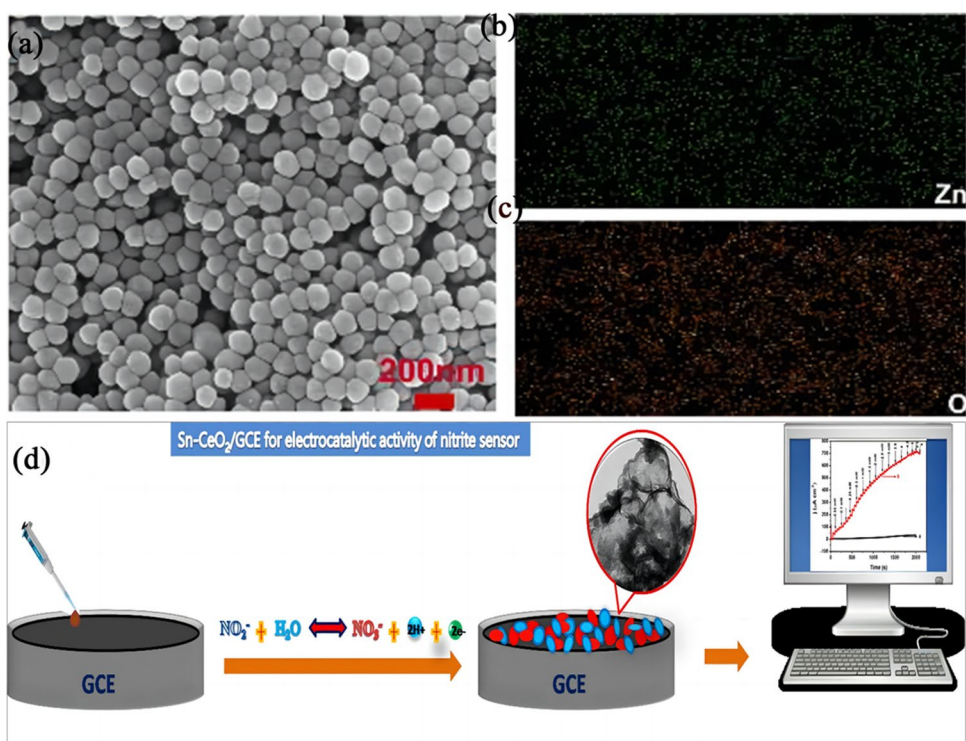
<sup>w</sup>Screen-printed fluorine-doped tin oxide electrode with activated jute carbon paste

<sup>x</sup>Copper ion-crosslinked bovine serum albumin nanoflower networks

The mixed solvents were synthesized by using polyethylene glycol 400 with water in a volume ratio of 12:1. Unlike other reported transition metal oxide nanoparticles, this approximately spherical ZnO nanostructure had higher uniformity and better dispersion, and no self-aggregation occurs when the particles are small (Fig. 7a, b, c). Comparison of sensing performance of bare GCE and near-spherical ZnO/GCE by CV and CA techniques. The results showed that the current response values of the modified electrodes were significantly higher than those of the bare electrodes. In addition, ZnO-based sensors had a wide linear range, low detection

limits, and strong immunity to interference. Moreover, they showed a satisfactory recovery rate in the detection of actual samples. In conclusion, nearly spherical ZnO nanomaterials have a wide range of promising applications for detection and analysis. Besides, nanostructured CeO<sub>2</sub> is also widely used in various fields due to its good chemical and physical properties, superior reusability, and stability [162, 163]. However, the nanostructure CeO<sub>2</sub> has a wide band gap and relatively low conductivity. Therefore, it needs to be modified when used as a sensing material [164]. For example, Manibalan et al. successfully doped Sn with CeO<sub>2</sub> using a

**Fig. 7** **a** SEM image of highly dispersed near-spherical zinc oxide. Mapping of **b** element zinc and **c** element oxygen prepared in an optimal solvent (PEG 400 to water volume ratio of 12:1) [127]. Copyright 2022, Elsevier. **d** Schematic diagram of modified electrode preparation [125]. Copyright 2022, Elsevier



simple precipitation synthesis method (Fig. 7d) [125]. The doping of Sn improves charge transfer as well as exposes the CeO<sub>2</sub> metal oxide active region, which can improve the electrical conductivity of CeO<sub>2</sub> and make CeO<sub>2</sub> nanoparticles have better surface properties. Characterized by XRD, FTIR, and TEM techniques, the results showed that the morphology of the catalyst was spherical nanoparticle clumps with a particle size of 8.5 nm. The catalytic performance of Sn-CeO<sub>2</sub>/GCE was studied by the amperometry method for nitrite. The results showed that the sensor had a detection range of  $10 \times 10^{-6}$ – $6 \times 10^{-3}$  M and a detection limit of 16 nM. In short, the sensors have good prospects for application and development.

**Nitrite sensor based on metal oxide composite (excludes non-precious metals)**

The performance of single metal oxides is inferior to that of metal oxide composites when used as catalysts. Metal oxides can be compounded with carbon materials, conductive polymers, metal-organic frameworks, and other substances. The composite nanomaterials of reduced graphene oxide and Fe<sub>3</sub>O<sub>4</sub> have excellent catalytic and electrical properties and exhibit excellent electrocatalytic activity in electrochemical sensors. Bharath et al. used mechanochemical ball milling to prepare high-quality graphene nanosheets from graphite in the presence of KMnO<sub>4</sub> and aspartic acid [149]. After that, Fe<sub>3</sub>O<sub>4</sub>/RGO composites were successfully prepared by loading Fe<sub>3</sub>O<sub>4</sub> nanoparticles onto graphene using a simple

hydrothermal method. The Fe<sub>3</sub>O<sub>4</sub>-RGO nanocomposites were characterized using HRTEM images, and the results demonstrated that good Fe<sub>3</sub>O<sub>4</sub> nanoparticles were distributed on the surface of reduced graphene oxide sheets, with an average particle size of 90 nm. The Fe<sub>3</sub>O<sub>4</sub>-RGO nanocomposites were loaded into GCE, and the prepared sensor exhibited good electrocatalytic activity, wide detection range, and low detection limit for nitrite. Radhakrishnan et al. prepared Fe<sub>2</sub>O<sub>3</sub>/rGO composites by one-step hydrothermal method [165], since Fe<sub>2</sub>O<sub>3</sub> nanoparticles are well dispersed on the rGO surface and Fe<sub>2</sub>O<sub>3</sub> nanoparticles on both sides of rGO can limit the aggregation of rGO. Therefore, the composite has high specific surface area, good electrical conductivity, and good catalytic performance for the oxidation of nitrite (Fig. 8a–f). Sensor based on Fe<sub>2</sub>O<sub>3</sub>/rGO composites has a wide detection range (0.05–780 μM) and a low detection limit (0.015 μM). The sensor can be applied to the environment, food, and other fields. In addition, conductive polymers have excellent electrical conductivity and tunable organic functional groups for intermolecular interactions with different target analytes. To improve the long-term stability of the conductive polymer, inorganic materials can be added and compounded with the conductive polymer. For example, the synergistic effect of conductive polymers and metal oxides can also show greater electrochemical sensing capabilities. Qiu and Qu combined polyaniline with MnO<sub>2</sub> (Fig. 8g) [128]. The transition metal oxide manganese dioxide has a unique oxidation behavior at different electrochemical potentials when used as an electrochemical

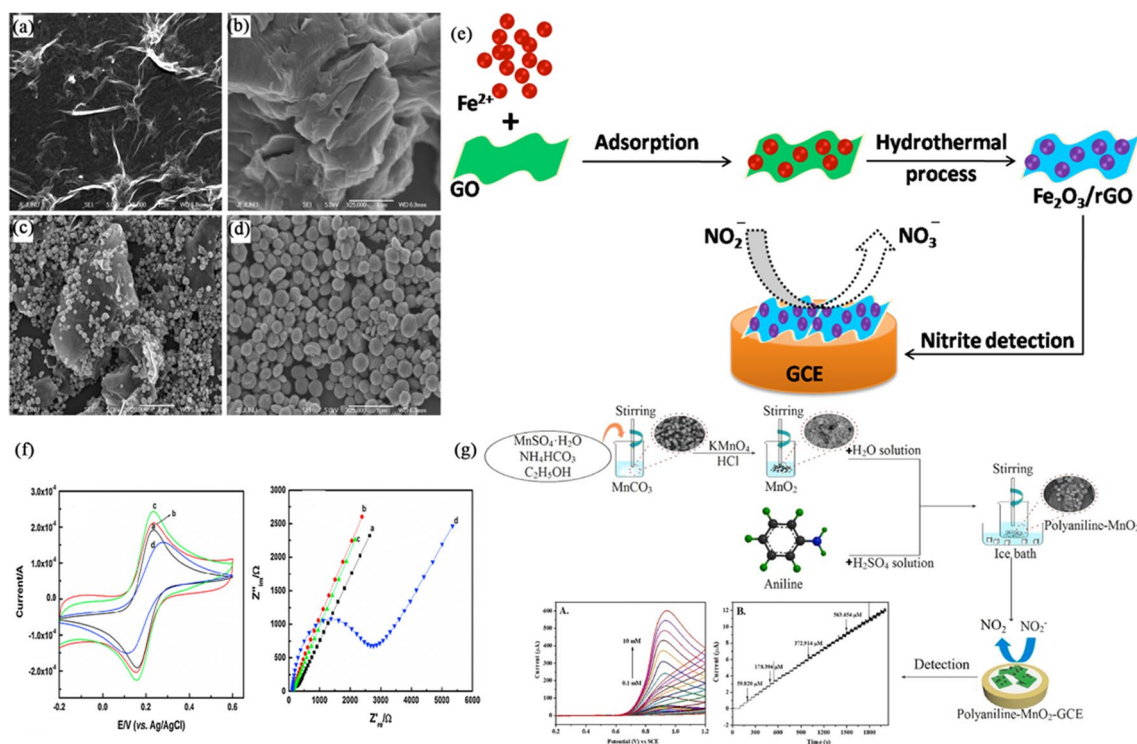


**Fig. 8** FE-SEM micrographs of **a** GO, **b** rGO, **c** Fe<sub>2</sub>O<sub>3</sub>/rGO, and **d** Fe<sub>2</sub>O<sub>3</sub>. **e** Nitrite detection scheme using Fe<sub>2</sub>O<sub>3</sub>/rGO-modified glassy carbon electrode. **f** CV behavior of the modified GC electrode in the presence of 1-mM [Fe(CN)<sub>6</sub>]<sup>3-/4-</sup> in 0.1-M KCl with a scan rate of 50 mV s<sup>-1</sup> and EIS behavior of the modified GC electrode by impedance measurement in the frequency range 100 KHz to 0.1 Hz at a DC

potential of 200 mV and an AC potential of ±10 mV in the presence of 1-mM [Fe(CN)<sub>6</sub>]<sup>3-/4-</sup> in 0.1-M KCl (curve a, bare GC; curve b, rGO; curve c, Fe<sub>2</sub>O<sub>3</sub>/rGO; curve d, Fe<sub>2</sub>O<sub>3</sub>-modified electrode) [165]. Copyright 2014, Elsevier. **g** Preparation of polyaniline-manganese dioxide organic-inorganic nanocomposites for nitrite electrochemical sensing [128]. Copyright 2022, Elsevier

sensing material. And the amine and imine groups in polyaniline contribute to the adsorption of nitrite on the nanocomposites. The morphology of MnCO<sub>3</sub>, MnO<sub>2</sub>, polyaniline, and polyaniline-MnO<sub>2</sub> nanocomposites was characterized by scanning electron microscopy. The results showed that manganese carbonate was slightly spherical and manganese dioxide was also spherical and larger in size. And in the image of the composite material, block polyaniline can be seen and spherical manganese dioxide was wrapped around the polyaniline. Composite materials were used to modify GCEs to prepare nitrite sensors. The sensor has a low detection limit (CV of 4.38 μM, CA of 1.08 μM) and a wide linear range (CV of 0.1~10 mM, CA of 19.98~732.17 μM). In addition, the organic-inorganic nanocomposite exhibited excellent sensing performance in actual sample analysis.

## Nitrite sensor based on conductive polymer composite

Conductive polymers have been widely used since their inception in 1977 and are of particular importance in materials science [166, 167]. Conducting polymers are

increasingly used in the detection of analytes by voltammetry or amperometry due to their selectivity, sensitivity, and strong adhesion to electrode surfaces [168]. They are an excellent choice for developing and modifying highly sensitive electrochemical sensors. A review of the literature from 2015 to 2020 (Science Direct and Wiley websites) shows that the number of papers on conductive polymer-based sensors has been increasing over the past few years [166]. This section focuses on the application of conductive polymer composites in nitrite sensors, and some of the properties exhibited by the material in modified electrodes are summarized in Table 4.

Among the conducting polymers, polyaniline, polypyrrole, polyacetylene, and their derivatives have received great attention. Li et al. prepared a polythiophene derivative membrane-modified GCE by a one-step electropolymerization method to establish a nitrite sensor [177]. DTT is a molten bicyclic heterocyclic compound with a rigid planar frame and an extended π-conjugated electronic structure. The effect of PolyDTTF on the electrochemical oxidation of nitrite was studied. The results showed that PolyDTTF had good electrical conductivity and enhanced electrocatalytic activity, which can greatly improve the electron transfer kinetics and



**Table 4** Electrochemical nitrite sensor based on conductive polymer

Electrode material	Method	Linear range ( $\mu\text{M}$ )	LOD ( $\mu\text{M}$ )	Sample	Ref.
PEDOT/NU-902/FTO	Amp	Up to 1600	1.71	–	[169]
PPy/UiO-66/GCE	Amp	0.05–1055.5	0.037	–	[122]
Poly(3ABA)/GCE	DPV	10–140	0.15	Human serum, orange juice	[170]
PolyNiCo_GCE	Amp	2.49–1700	0.45	Tap water	[171]
CQD_PEDOT/GCE	Amp	0.50–1110	0.088	–	[172]
CG/PPy/CS/GCE	DPV	0.2–1000	0.02	Water	[173]
PDAP-NiHCF/GCE	Amp	0.1–130	0.0151	Water and ham sausage	[174]
PPy-Cunano/GCE	Amp	0.1–0.7, 0.7–1040.7	0.03	Well and lake water	[175]
CuNPs/3D-PANI/H/GCE	Amp	0.2–4300	0.07	Lake water and milk	[176]
PolyDTTF/GCE	Amp	0.0055–35	0.002	Ham, sauce beef, and pickle	[177]
Co/PPy/GCE	Amp	2–3318	0.35	Pickled Chinese cabbage	[23]

facilitate the oxidation of nitrite. In addition to this, sensors based on this material had significant detection limits and good detection ranges. The reason may be that PolyDTTF has high electron affinity and synergistic effect, which enables rapid adsorption of analytes to the electrode surface. In conclusion, the preparation method is simple, the film thickness can be controlled, and the sensor can be used for detection in real samples. The sensor offers the possibility of application in the food industry and environmental analysis. Since it is challenging to synthesize a single polymer to meet multiple requirements in the practical application of nitrite detection. Therefore, composites are often used to modify the electrodes. Generally, conducting polymers are often compounded with metal nanoparticles, carbon-based nanomaterials, metal-organic framework chemicals, and other substances. For example, Lu et al. successfully synthesized Co/PPy nanocone composites by compounding metallic cobalt with conductive polymer PPy by electrodeposition technique [23]. Polypyrrole has excellent electrochemical stability and high electrical conductivity compared to other conductive polymers. It can be used as an attachment substrate for various metal nanomaterials. Due to the synergistic effect of nanocomposite components, the composite material has the advantages of high sensitivity, high capacitance, and controllable conductivity. Because its three-dimensional structure provides more active sites for nitrite detection, the composite exhibits good nitrite determination performance in electrochemical studies. Carboxyl graphene is a two-dimensional crystalline carbon material that has received great attention in practice due to its excellent properties. Xiao et al. prepared composites of CG (carboxyl graphene), PPy, and CS (chitosan) nanocomposites [173]. For CS is rich in amino groups, it can attract negatively charged nitrite. The recombination of PPy and CG provides a large specific surface area and numerous active sites. In conclusion, the composite material can improve the selectivity and sensitivity of nitrite determination. In addition, DPV is used for electrochemical performance testing. The results showed

that the detection range of the composite-modified sensor was 0.2~1000  $\mu\text{M}$ , and the detection limit was 0.02  $\mu\text{M}$ . The sensor has a promising application in the practical detection of nitrite. Saho et al. synthesized fibrous nanocomposites of reduced graphene oxide, manganese ferrite, and polyaniline (RGO/MnFe<sub>2</sub>O<sub>4</sub>/polyaniline) in a two-step process [63]. The introduction of RGO not only prevents the agglomeration of MnFe<sub>2</sub>O<sub>4</sub> nanoparticles and increases the specific surface area but also helps to accelerate the electron transfer process from reduced graphene oxide flakes to MnFe<sub>2</sub>O<sub>4</sub> nanoparticles. In addition, the strong interaction between graphene and polyaniline allows for uninterrupted charge flow during nitrite oxidation (Fig. 9). The electrode modified based on this composite has a wide linear range (0.05~12,000  $\mu\text{M}$ ) and a low detection limit (0.015  $\mu\text{M}$ ), which can be used for the detection of nitrite in rain water samples.

## Conclusion and outlook

This paper reviews the research progress and application status of nitrite electrochemical sensors based on four nanomaterials. The characteristics and advantages of carbon nanomaterials (graphene, carbon nanotubes), metal-organic frameworks, non-precious metals, and conducting polymers are systematically introduced in nitrite electrochemical sensors. These materials have been extensively studied for their unique and fascinating properties (e.g., graphene has large specific surface area and inexpensive and readily available raw materials, metal-organic frameworks with high porosity and tunable pore size). However, individual materials also have some disadvantages, which leads to the performance in nitrite detection often inferior to that of composite materials. Many studies have shown that the synergistic effect of composites not only improves stability and accelerates the electron transfer rate but also provides more active sites in the detection of nitrite. Although the field has achieved great results over the course of decades of development.

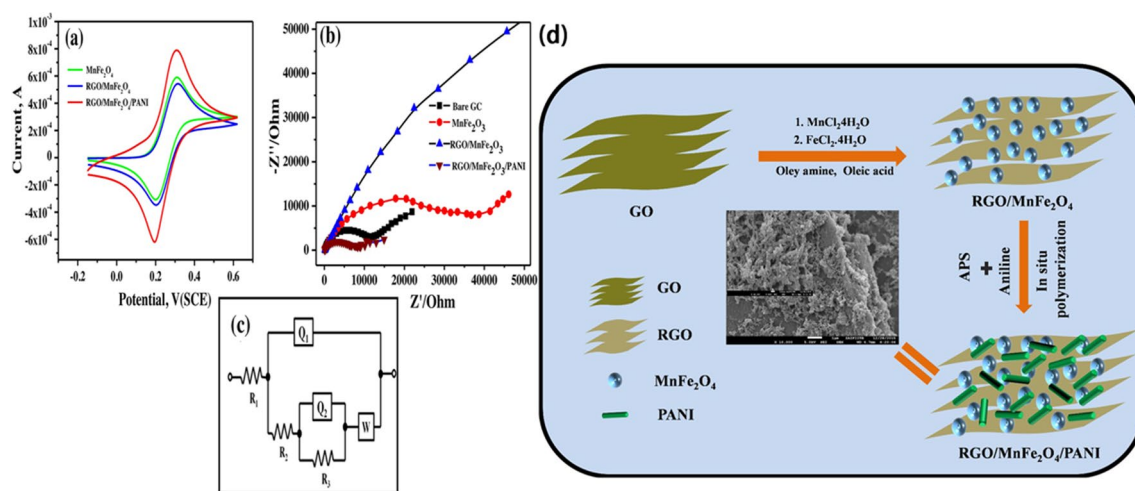


**Fig. 9** **a** Ferrocyanide cyclic voltammetry of electrodes modified with different modifiers in a 0.1-M phosphate buffer at pH 7. **b** Nyquist diagram recorded by modifying the electrode with different modifiers at an excitation potential of 0.3 V in a 0.1-M phosphate buffer at

pH 7. **c** Equivalent circuit used for the fitting of the impedance plot. **d** The synthesis procedure adopted to synthesize the nanocomposite material [63]. Copyright 2020, Elsevier

However, further research on electrochemical nitrite sensors still faces many challenges. The morphology, purity, and dispersion of carbon nanomaterials have great influence on the electrocatalytic performance. It is necessary to seek new synthesis methods or consider three-dimensional structures. In addition, the carbon nanomaterials will peel off the electrode surface, which will affect the stability of the sensor and limit its further development in the long-term detection of nitrite. Therefore, it is necessary to study more robust fixing methods. Due to the poor structural stability and conductivity of MOF materials, the sensor is not ideal for nitrite detection. Developing functional MOF composites remains a challenge. In addition, the synthesis process of MOF composites that has been studied is too complex to achieve large-scale production, so it is still necessary to explore new synthesis paths. As far as metal materials are concerned, the electrocatalytic performance of precious metals is better than that of non-precious metals, so it is still a difficult problem to find non-precious metals that can replace precious metals. At present, there are few electrochemical methods on the combination of conductive polymers with carbon nanomaterials and metal materials. So it can be considered to combine conductive polymers with other materials to further improve the electrocatalytic performance. In general, the first is the preparation method; the preparation of nanomaterials involves precise and targeted control of the shape and size of the nanomaterials in most cases. Different preparation methods often affect the performance of the catalyst size. In addition to this, most sensors are manufactured on rigid substrates, resulting in a lack of flexibility in the sensors. Second, when designing a catalyst with excellent performance, it is necessary to explain the reaction process

and mechanism on the catalyst. In principle, the catalytic performance of a catalyst is determined by its electronic structure, while the true catalytic active site and the exact reaction mechanism of some materials are still unclear. Finally, in most cases, nitrite electrochemical sensors have the disadvantages of high cost of large-scale preparation, time-consuming synthesis process, and threats to humans and the environment of nanomaterials. These disadvantages limit the practical application of the sensor.

For future research on nitrite electrochemical sensors, the following aspects can be considered. First, research should focus on new synthetic methods to change the structure and composition of catalysts in order to adjust their electronic structure. And new nanomaterials can be combined with good conductive polymers. In addition to this, low-cost, biocompatible materials and more environmentally friendly synthesis methods and equipment should be used. Second, the reaction mechanism of nitrite sensors is further explored, and the true catalytic active sites of various materials are clarified. This results in higher sensitivity and better selectivity of nitrite electrochemical sensors. Finally, technologies such as screen printing, ARM microcontrollers, and mobile intelligence can be combined to build portable  $\text{NO}_2^-$  electrochemical sensors to achieve remote real-time measurement of nitrite content. And existing nitrite sensors can be integrated into nutrient management programs in agroecosystems to facilitate rapid and accurate detection of spatial and temporal changes in nitrite levels in soil.

**Availability of data and materials** This declaration is “not applicable.”

**Author contributions** Jie Zhang: had the idea for the article, critically revised. Jing-He Yang: had the idea for the article, critically revised.

Tingting Zhang: critically revised. Yu-Xi Yang: performed the literature search and data analysis, write a first draft.

**Funding** This study was supported by the National Natural Science Foundation of China (Grant Nos. 21706241, U1404503, 21403053), China Post-doctoral Science Foundation (2020M672305, 2018M642791), and Key Scientific and Technological Project of Henan Province (202102210042).

## Declarations

**Ethical approval** This declaration is “not applicable.”

**Competing interests** The authors declare no competing interests.

## References

- Dai L, Chang DW, Baek JB et al (2012) Carbon nanomaterials for advanced energy conversion and storage. *Small* 8(8):1130–1166. <https://doi.org/10.1002/sml.201101594>
- Li D, Wang T, Li Z et al (2019) Application of graphene-based materials for detection of nitrate and nitrite in water—a review. *Sensors (Basel)* 20(1):54. <https://doi.org/10.3390/s20010054>
- Zhang J, Zhang T, Yang J-H (2022) Precious metal nanomaterial-modified electrochemical sensors for nitrite detection. *Ionics* 28(5):2041–2064. <https://doi.org/10.1007/s11581-022-04509-3>
- Amali RKA, Lim HN, Ibrahim I et al (2021) Significance of nanomaterials in electrochemical sensors for nitrate detection: a review. *Trends Environ Anal Chem* 31:e00135. <https://doi.org/10.1016/j.teac.2021.e00135>
- Donnelly-Greenan EL, Nevins HM, Harvey JT (2019) Entangled seabird and marine mammal reports from citizen science surveys from coastal California (1997–2017). *Mar Pollut Bull* 149:110557. <https://doi.org/10.1016/j.marpolbul.2019.110557>
- Li X, Ping J, Ying Y (2019) Recent developments in carbon nanomaterial-enabled electrochemical sensors for nitrite detection. *TrAC Trends Anal Chem* 113:1–12. <https://doi.org/10.1016/j.trac.2019.01.008>
- Hatta M, Ruzicka JJ, Measures CI (2020) The performance of a new linear light path flow cell is compared with a liquid core waveguide and the linear cell is used for spectrophotometric determination of nitrite in sea water at nanomolar concentrations. *Talanta* 219:121240. <https://doi.org/10.1016/j.talanta.2020.121240>
- Mao Y, Bao Y, Han D-X et al (2018) Research progress on nitrite electrochemical sensor. *Chin J Anal Chem* 46(2):147–155. [https://doi.org/10.1016/s1872-2040\(17\)61066-1](https://doi.org/10.1016/s1872-2040(17)61066-1)
- Wu J, Wang X, Lin Y et al (2016) Peroxynitrous-acid-induced chemiluminescence detection of nitrite based on microfluidic chip. *Talanta* 154:73–79. <https://doi.org/10.1016/j.talanta.2016.03.062>
- Kodamatani H, Yamazaki S, Saito K et al (2009) Selective determination method for measurement of nitrite and nitrate in water samples using high-performance liquid chromatography with post-column photochemical reaction and chemiluminescence detection. *J Chromatogr A* 1216(15):3163–3167. <https://doi.org/10.1016/j.chroma.2009.01.096>
- Chamandust S, Mehrasebi MR, Kamali K et al (2016) Simultaneous determination of nitrite and nitrate in milk samples by ion chromatography method and estimation of dietary intake. *Int J Food Prop* 19(9):1983–1993. <https://doi.org/10.1080/10942912.2015.1091007>
- Fu Y, Bian C, Kuang J et al (2015) A palladium-tin modified microband electrode array for nitrate determination. *Sensors (Basel)* 15(9):23249–23261. <https://doi.org/10.3390/s150923249>
- Kalaycıoğlu Z, Erım FB (2015) Simultaneous determination of nitrate and nitrite in fish products with improved sensitivity by sample stacking-capillary electrophoresis. *Food Anal Methods* 9(3):706–711. <https://doi.org/10.1007/s12161-015-0241-4>
- Xu Z, Shi W, Yang C et al (2020) A colorimetric fluorescent probe for rapid and specific detection of nitrite. *Luminescence* 35(2):299–304. <https://doi.org/10.1002/bio.3727>
- Bagheri H, Hajian A, Rezaei M et al (2017) Composite of Cu metal nanoparticles-multiwall carbon nanotubes-reduced graphene oxide as a novel and high performance platform of the electrochemical sensor for simultaneous determination of nitrite and nitrate. *J Hazard Mater* 324(Pt B):762–772. <https://doi.org/10.1016/j.jhazmat.2016.11.055>
- Yang J-H, Yang H, Liu S et al (2015) Microwave-assisted synthesis graphite-supported Pd nanoparticles for detection of nitrite. *Sensors Actuators B Chem* 220:652–658. <https://doi.org/10.1016/j.snb.2015.05.118>
- Kanoun O, Lazarevic-Pasti T, Pasti I et al (2021) A review of nanocomposite-modified electrochemical sensors for water quality monitoring. *Sensors (Basel)* 21(12):4131. <https://doi.org/10.3390/s21124131>
- Rassaei L, Marken F, Sillanpää M et al (2011) Nanoparticles in electrochemical sensors for environmental monitoring. *TrAC Trends Anal Chem* 30(11):1704–1715. <https://doi.org/10.1016/j.trac.2011.05.009>
- Li T, Shang D, Gao S et al (2022) Two-dimensional material-based electrochemical sensors/biosensors for food safety and biomolecular detection. *Biosensors (Basel)* 12(5):314. <https://doi.org/10.3390/bios12050314>
- Dou B, Yan J, Chen Q et al (2021) Development of an innovative nitrite sensing platform based on the construction of carbon-layer-coated In<sub>2</sub>O<sub>3</sub> porous tubes. *Sensors Actuators B Chem* 328:129082. <https://doi.org/10.1016/j.snb.2020.129082>
- Li G, Xia Y, Tian Y et al (2019) Review—recent developments on graphene-based electrochemical sensors toward nitrite. *J Electrochem Soc* 166(12):B881–B895. <https://doi.org/10.1149/2.0171912jes>
- Cheng Z, Song H, Zhang X et al (2022) Enhanced non-enzyme nitrite electrochemical sensing property based on stir bar-shaped ZnO nanorods decorated with nitrogen-doped reduced graphene oxide. *Sensors Actuators B Chem* 355:131313. <https://doi.org/10.1016/j.snb.2021.131313>
- Lu H, Wang H, Yang L et al (2021) A sensitive electrochemical sensor based on metal cobalt wrapped conducting polymer polypyrrole nanocone arrays for the assay of nitrite. *Mikrochim Acta* 189(1):26. <https://doi.org/10.1007/s00604-021-05131-2>
- Madasamy T, Pandiaraj M, Balamurugan M et al (2014) Copper, zinc superoxide dismutase and nitrate reductase coimmobilized bienzymatic biosensor for the simultaneous determination of nitrite and nitrate. *Biosens Bioelectron* 52:209–215. <https://doi.org/10.1016/j.bios.2013.08.036>
- Salagare S, Adarakatti PS, Venkataramanappa Y et al (2021) Electrochemical nitrite sensing employing palladium oxide-reduced graphene oxide (PdO-RGO) nanocomposites: application to food and environmental samples. *Ionics* 28(2):927–938. <https://doi.org/10.1007/s11581-021-04355-9>
- Salagare S, Adarakatti PS, Yarradoddappa V (2021) Facile synthesis of silver nanoparticle-decorated zinc oxide nanocomposite-based pencil graphite electrode for selective electrochemical determination of nitrite. *Carbon Letters* 31(6):1273–1286. <https://doi.org/10.1007/s42823-021-00251-4>
- Umamathi R, Venkateswara Raju C, Majid Ghoreishian S et al (2022) Recent advances in the use of graphitic carbon

- nitride-based composites for the electrochemical detection of hazardous contaminants. *Coord Chem Rev* 470:214708. <https://doi.org/10.1016/j.ccr.2022.214708>
28. Moyo M, Mudarikwa P, Shumba M et al (2017) Voltammetric sensing of nitrite in aqueous solution using titanium dioxide anchored multiwalled carbon nanotubes. *Ionics* 24(8):2489–2498. <https://doi.org/10.1007/s11581-017-2358-5>
  29. Liu H-Y, Wen J-J, Huang Z-H et al (2019) Prussian blue analogue of copper-cobalt decorated with multi-walled carbon nanotubes based electrochemical sensor for sensitive determination of nitrite in food samples. *Chin J Anal Chem* 47(6):e19066–e19072. [https://doi.org/10.1016/s1872-2040\(19\)61168-0](https://doi.org/10.1016/s1872-2040(19)61168-0)
  30. Zhu D, Zhen Q, Xin J et al (2020) A free-standing and flexible phosphorus/nitrogen dual-doped three-dimensional reticular porous carbon frameworks encapsulated cobalt phosphide with superior performance for nitrite detection in drinking water and sausage samples. *Sensors Actuators B Chem* 321:128541. <https://doi.org/10.1016/j.snb.2020.128541>
  31. Xian H, Wang P, Zhou Y et al (2010) Electrochemical determination of nitrite via covalent immobilization of a single-walled carbon nanotubes and single stranded deoxyribonucleic acid nanocomposite on a glassy carbon electrode. *Microchim Acta* 171(1-2):63–69. <https://doi.org/10.1007/s00604-010-0404-3>
  32. Yang S, Xia B, Zeng X et al (2010) Fabrication of DNA functionalized carbon nanotubes/Cu<sup>2+</sup> complex by one-step electrodeposition and its sensitive determination of nitrite. *Anal Chim Acta* 667(1-2):57–62. <https://doi.org/10.1016/j.aca.2010.03.063>
  33. Salhi O, Ez-Zine T, Oularbi L et al (2022) Electrochemical sensing of nitrite ions using modified electrode by poly 1,8-diaminonaphthalene/functionalized multi-walled carbon nanotubes. *Front Chem* 10:870393. <https://doi.org/10.3389/fchem.2022.870393>
  34. Atta NF, Galal A, Ahmed YM et al (2021) Development of an innovative nitrite sensing platform based on the construction of an electrochemical composite sensor of polymer coated CNTs and decorated with magnetite nanoparticles. *Electroanalysis* 33(6):1510–1519. <https://doi.org/10.1002/elan.202060598>
  35. Rashed MA, Faisal M, Alsaiani M et al (2021) MWCNT-doped polypyrrole-carbon black modified glassy carbon electrode for efficient electrochemical sensing of nitrite ions. *Electrocatalysis* 12(6):650–666. <https://doi.org/10.1007/s12678-021-00675-6>
  36. Chen Y, Waterhouse GIN, Qiao X et al (2022) Sensitive analytical detection of nitrite using an electrochemical sensor with STAB-functionalized Nb<sub>2</sub>C@MWCNTs for signal amplification. *Food Chem* 372:131356. <https://doi.org/10.1016/j.foodchem.2021.131356>
  37. Lu S, Hummel M, Kang S et al (2020) Selective voltammetric determination of nitrite using cobalt phthalocyanine modified on multiwalled carbon nanotubes. *J Electrochem Soc* 167(4):046515. <https://doi.org/10.1149/1945-7111/ab7982>
  38. Mounesh and K. R. Venugopala Reddy (2020) Sensitive and reliable electrochemical detection of nitrite and H<sub>2</sub>O<sub>2</sub> embellish-CoPc coupled with appliance of composite MWCNTs. *Anal Chim Acta* 1108:98–107. <https://doi.org/10.1016/j.aca.2020.02.057>
  39. Annalakshmi M, Balasubramanian P, Chen SM et al (2018) Amperometric sensing of nitrite at nanomolar concentrations by using carboxylated multiwalled carbon nanotubes modified with titanium nitride nanoparticles. *Mikrochim Acta* 186(1):8. <https://doi.org/10.1007/s00604-018-3136-4>
  40. Rebiś T, Falkowski M, Kryjewski M et al (2019) Single-walled carbon nanotube/sulfanyl porphyrazine hybrids deposited on glassy carbon electrode for sensitive determination of nitrites. *Dyes Pigment* 171:107660. <https://doi.org/10.1016/j.dyepig.2019.107660>
  41. Sudha V, Senthil Kumar SM, Thangamuthu R (2018) Simultaneous electrochemical sensing of sulphite and nitrite on acid-functionalized multi-walled carbon nanotubes modified electrodes. *J Alloys Compd* 749:990–999. <https://doi.org/10.1016/j.jallcom.2018.03.287>
  42. Arulraj AD, Sundaram E, Vasantha VS et al (2018) Polypyrrole with a functionalized multi-walled carbon nanotube hybrid nanocomposite: a new and efficient nitrite sensor. *New J Chem* 42(5):3748–3757. <https://doi.org/10.1039/c7nj04130f>
  43. Lin XR, Zheng YF, Song XC (2018) Fe<sub>2</sub>O<sub>3</sub>/MWCNTs nanocomposite decorated glassy carbon electrode for the determination of nitrite. *Bull Mater Sci* 41(2):35. <https://doi.org/10.1007/s12034-018-1553-y>
  44. Zhu F, Shi H, Wang C et al (2021) Disposable carbon electrodes modified by a bismuth selenide/carboxylic multiwalled carbon nanotubes composite for the effective electrocatalytic analysis of nitrite. *Sensors Actuators B Chem* 332:129454. <https://doi.org/10.1016/j.snb.2021.129454>
  45. Brahem A, Al-Hamry A, Gross MA et al (2022) Stability enhancement of laser-scribed reduced graphene oxide electrodes functionalized by iron oxide/reduced graphene oxide nanocomposites for nitrite sensors. *J Compos Sci* 6(8):221. <https://doi.org/10.3390/jcs6080221>
  46. Paisanpisuttisin A, Poonwattanapong P, Rakthabut P et al (2022) Sensitive electrochemical sensor based on nickel/PDDA/reduced graphene oxide modified screen-printed carbon electrode for nitrite detection. *RSC Adv* 12(45):29491–29502. <https://doi.org/10.1039/d2ra03918d>
  47. Yuan X, Chen J, Ling Y et al (2022) A facile and efficient nitrite electrochemical sensor based on N, O co-doped porous graphene film. *Microchem J* 178:107361. <https://doi.org/10.1016/j.micro.2022.107361>
  48. Sookhakian M, Mat Teridi MA, Tong GB et al (2021) Reduced graphene oxide/copper nanoparticle composites as electrochemical sensor materials for nitrate detection. *ACS Appl Nano Mater* 4(11):12737–12744. <https://doi.org/10.1021/acsanm.1c03351>
  49. Suma BP, Pandurangappa M (2019) Graphene oxide/copper terephthalate composite as a sensing platform for nitrite quantification and its application to environmental samples. *J Solid State Electrochem* 24(1):69–79. <https://doi.org/10.1007/s10008-019-04454-8>
  50. Tajiki A, Abdouss M, Sadjadi S et al (2020) Voltammetric detection of nitrite anions employing imidazole functionalized reduced graphene oxide as an electrocatalyst. *Electroanalysis* 32(10):2290–2298. <https://doi.org/10.1002/elan.202060187>
  51. Madhuvilakku R, Alagar S, Mariappan R et al (2020) Glassy carbon electrodes modified with reduced graphene oxide-MoS<sub>2</sub>-poly (3, 4-ethylene dioxythiophene) nanocomposites for the non-enzymatic detection of nitrite in water and milk. *Anal Chim Acta* 1093:93–105. <https://doi.org/10.1016/j.aca.2019.09.043>
  52. Saranya S, Deepa PN (2020) Evolution of novel rGO/ZrHCF composite and utility in electrocatalysis towards nanomolar detection of sodium nitrite and ferulic acid. *J Mater Sci Mater Electron* 31(21):18923–18936. <https://doi.org/10.1007/s10854-020-04430-3>
  53. Rashed MA, Faisal M, Harraz FA et al (2020) rGO/ZnO/Nafion nanocomposite as highly sensitive and selective amperometric sensor for detecting nitrite ions (NO<sub>2</sub><sup>-</sup>). *J Taiwan Inst Chem Eng* 112:345–356. <https://doi.org/10.1016/j.jtice.2020.05.015>
  54. Ahammad AJS, Alam MK, Islam T et al (2020) Poly (brilliant cresyl blue)-reduced graphene oxide modified activated GCE for nitrite detection: analyzing the synergistic interactions through experimental and computational study. *Electrochim Acta* 349:136375. <https://doi.org/10.1016/j.electacta.2020.136375>
  55. Zhao Z, Zhang J, Wang W et al (2019) Synthesis and electrochemical properties of Co<sub>3</sub>O<sub>4</sub>-rGO/CNTs composites towards highly sensitive nitrite detection. *Appl Surf Sci* 485:274–282. <https://doi.org/10.1016/j.apsusc.2019.04.202>

56. Li Y, Cheng C, Yang Y et al (2019) A novel electrochemical sensor based on CuO/H-C<sub>3</sub>N<sub>4</sub>/rGO nanocomposite for efficient electrochemical sensing nitrite. *J Alloys Compd* 798:764–772. <https://doi.org/10.1016/j.jallcom.2019.05.137>
57. Rostami M, Abdi G, Kazemi SH et al (2019) Nanocomposite of magnetic nanoparticles/graphene oxide decorated with acetic acid moieties on glassy carbon electrode: a facile method to detect nitrite concentration. *J Electroanal Chem* 847:113239. <https://doi.org/10.1016/j.jelechem.2019.113239>
58. Li L, Liu H, Li B et al (2019) Design and construction of polyaniline/reduced graphene oxide three-dimensional dendritic architecture on interdigital electrode for sensitive detection nitrite. *Macromol Res* 28(5):455–464. <https://doi.org/10.1007/s13233-020-8062-8>
59. Suma BP, Adarakatti PS, Kempahnumakkagari SK et al (2019) A new polyoxometalate/rGO/Pani composite modified electrode for electrochemical sensing of nitrite and its application to food and environmental samples. *Mater Chem Phys* 229:269–278. <https://doi.org/10.1016/j.matchemphys.2019.02.087>
60. Zhang J, Zhang Y, Zhou J et al (2018) Construction of a highly sensitive non-enzymatic nitrite sensor using electrochemically reduced holey graphene. *Anal Chim Acta* 1043:28–34. <https://doi.org/10.1016/j.aca.2018.08.045>
61. Hu J, Zhang J, Zhao Z et al (2017) Synthesis and electrochemical properties of rGO-MoS<sub>2</sub> heterostructures for highly sensitive nitrite detection. *Ionics* 24(2):577–587. <https://doi.org/10.1007/s11581-017-2202-y>
62. Wang Y, Cao W, Yin C et al (2018) Nonenzymatic amperometric sensor for nitrite detection based on a nanocomposite consisting of nickel hydroxide and reduced graphene oxide. *Electroanalysis* 30(12):2916–2924. <https://doi.org/10.1002/elan.201800627>
63. Sahoo S, Sahoo PK, Sharma A et al (2020) Interfacial polymerized RGO/MnFe<sub>2</sub>O<sub>4</sub>/polyaniline fibrous nanocomposite supported glassy carbon electrode for selective and ultrasensitive detection of nitrite. *Sensors Actuators B Chem* 309:127763. <https://doi.org/10.1016/j.snb.2020.127763>
64. Yue X, Luo X, Zhou Z et al (2019) pH-regulated synthesis of CuOx/ERGO nanohybrids with tunable electrocatalytic oxidation activity towards nitrite sensing. *New J Chem* 43(12):4947–4958. <https://doi.org/10.1039/c9nj00474b>
65. Wang S, Liu M, He S et al (2018) Protonated carbon nitride induced hierarchically ordered Fe<sub>2</sub>O<sub>3</sub>/H C<sub>3</sub>N<sub>4</sub>/rGO architecture with enhanced electrochemical sensing of nitrite. *Sensors Actuators B Chem* 260:490–498. <https://doi.org/10.1016/j.snb.2018.01.073>
66. Zhang G, Pan P, Yang Z et al (2020) Rapid synthesis of cypress-like CuO nanomaterials and CuO/MWCNTs composites for ultrahigh sensitivity electrochemical sensing of nitrite. *Microchem J* 159:105439. <https://doi.org/10.1016/j.microc.2020.105439>
67. Govindasamy M, Wang SF, Huang CH et al (2022) Colloidal synthesis of perovskite-type lanthanum aluminate incorporated graphene oxide composites: electrochemical detection of nitrite in meat extract and drinking water. *Microchim Acta* 189(5):210. <https://doi.org/10.1007/s00604-022-05296-4>
68. Yılmaz-Alhan B, Çelik G, Oguzhan Caglayan M et al (2022) Determination of nitrite on manganese dioxide doped reduced graphene oxide modified glassy carbon by differential pulse voltammetry. *Chem Pap* 76(8):4919–4925. <https://doi.org/10.1007/s11696-022-02218-9>
69. Yue X, Li Y, Li M et al (2021) Three-dimensional porous carbon derived from different organic acid salts for application in electrochemical sensing. *RSC Adv* 11(50):31834–31844. <https://doi.org/10.1039/d1ra05105a>
70. Liu Q, Zhang B, Du S et al (2020) Porous hollow carbon nanospheres as a novel sensing platform for sensitive detection of nitrite in pickle directly. *J Appl Electrochem* 51(2):295–306. <https://doi.org/10.1007/s10800-020-01501-5>
71. Alsaiani M, Saleem A, Alsaiani R et al (2022) SiO<sub>2</sub>/Al<sub>2</sub>O<sub>3</sub>/C grafted 3-n propylpyridinium silsesquioxane chloride-based non-enzymatic electrochemical sensor for determination of carcinogenic nitrite in food products. *Food Chem* 369:130970. <https://doi.org/10.1016/j.foodchem.2021.130970>
72. Dong X, Xie S, Zhu J et al (2021) Mesoporous CoOx/C nanocomposites functionalized electrochemical sensor for rapid and continuous detection of nitrite. *Coatings* 11(5):596. <https://doi.org/10.3390/coatings11050596>
73. Zhang Y, Zhu W, Wang Y et al (2019) High-performance electrochemical nitrite sensing enabled using commercial carbon fiber cloth. *Inorg Chem Front* 6(6):1501–1506. <https://doi.org/10.1039/c9qi00255c>
74. Sivakumar M, Sakthivel M, Chen S-M et al (2017) An electrochemical selective detection of nitrite sensor for polyaniline doped graphene oxide modified electrode. *Int J Electrochem Sci* 12(6):4835–4846. <https://doi.org/10.20964/2017.06.24>
75. Salagare S, Adarakatti PS, Almalki ASA et al (2022) An efficient electrochemical sensor for nitrite based on a mesoporous nickel cobaltite-reduced graphene oxide (NiCo-RGO) nanocomposite. *Mater Res Innov* 27(4):212–222. <https://doi.org/10.1080/14328917.2022.2113678>
76. Gligor D, Walcarius A (2014) Glassy carbon electrode modified with a film of poly(toluidine blue O) and carbon nanotubes for nitrite detection. *J Solid State Electrochem* 18(6):1519–1528. <https://doi.org/10.1007/s10008-013-2365-z>
77. Zhang D, Ma H, Chen Y et al (2013) Amperometric detection of nitrite based on Dawson-type vanadotungstophosphate and carbon nanotubes. *Anal Chim Acta* 792:35–44. <https://doi.org/10.1016/j.aca.2013.07.010>
78. Zhou L, Wang J-P, Gai L et al (2013) An amperometric sensor based on ionic liquid and carbon nanotube modified composite electrode for the determination of nitrite in milk. *Sensors Actuators B Chem* 181:65–70. <https://doi.org/10.1016/j.snb.2013.02.041>
79. Moheimanian N, Raouf JB, Safavi A et al (2013) Nitrite electrochemical sensor for food analysis based on direct immobilization of hemoglobin on multi-walled carbon nanotube ionic liquid electrode. *J Iran Chem Soc* 11(4):1217–1222. <https://doi.org/10.1007/s13738-013-0391-5>
80. Majidi MR, Naseri A, Panahian S et al (2013) Electrocatalytic oxidation and determination of nitrite at multi-walled carbon nanotubes modified carbon ceramic electrode. *J Chin Chem Soc* 60(3):314–320. <https://doi.org/10.1002/jccs.201200365>
81. Mani V, Wu T-Y, Chen S-M (2013) Iron nanoparticles decorated graphene-multiwalled carbon nanotubes nanocomposite-modified glassy carbon electrode for the sensitive determination of nitrite. *J Solid State Electrochem* 18(4):1015–1023. <https://doi.org/10.1007/s10008-013-2349-z>
82. Xu F, Deng M, Liu Y et al (2014) Facile preparation of poly(diallyldimethylammonium chloride) modified reduced graphene oxide for sensitive detection of nitrite. *Electrochem Commun* 47:33–36. <https://doi.org/10.1016/j.elecom.2014.07.016>
83. Liu M, Wang L, Meng Y et al (2014) (4-Ferrocenylethyne) phenylamine functionalized graphene oxide modified electrode for sensitive nitrite sensing. *Electrochim Acta* 116:504–511. <https://doi.org/10.1016/j.electacta.2013.11.060>
84. Gholivand MB, Jalalvand AR, Goicoechea HC (2014) Computer-assisted electrochemical fabrication of a highly selective and sensitive amperometric nitrite sensor based on surface decoration of electrochemically reduced graphene oxide nanosheets with CoNi bimetallic alloy nanoparticles. *Mater Sci Eng C* 40:109–120. <https://doi.org/10.1016/j.msec.2014.03.044>
85. Zhang D, Fang Y, Miao Z et al (2013) Direct electrodeposition of reduced graphene oxide and dendritic copper nanoclusters on glassy carbon electrode for electrochemical detection of nitrite.

- Electrochim Acta 107:656–663. <https://doi.org/10.1016/j.electacta.2013.06.015>
86. Yang YJ, Li W (2014) CTAB functionalized graphene oxide/multiwalled carbon nanotube composite modified electrode for the simultaneous determination of ascorbic acid, dopamine, uric acid and nitrite. *Biosens Bioelectron* 56:300–306. <https://doi.org/10.1016/j.bios.2014.01.037>
87. Wang J, Yin G, Shao Y et al (2008) Electrochemical durability investigation of single-walled and multi-walled carbon nanotubes under potentiostatic conditions. *J Power Sources* 176(1):128–131. <https://doi.org/10.1016/j.jpowsour.2007.10.057>
88. Yang Z, Zhong Y, Zhou X et al (2022) Metal-organic framework-based sensors for nitrite detection: a short review. *J Food Meas Charact* 16(2):1572–1582. <https://doi.org/10.1007/s11694-021-01270-5>
89. Saraf M, Rajak R, Mobin SM (2016) A fascinating multitasking Cu-MOF/rGO hybrid for high performance supercapacitors and highly sensitive and selective electrochemical nitrite sensors. *J Mater Chem A* 4(42):16432–16445. <https://doi.org/10.1039/c6ta06470a>
90. Ping J, Zhou Y, Wu Y et al (2015) Recent advances in aptasensors based on graphene and graphene-like nanomaterials. *Biosens Bioelectron* 64:373–385. <https://doi.org/10.1016/j.bios.2014.08.090>
91. Mehmeti E, Stankovic DM, Hajrizi A et al (2016) The use of graphene nanoribbons as efficient electrochemical sensing material for nitrite determination. *Talanta* 159:34–39. <https://doi.org/10.1016/j.talanta.2016.05.079>
92. Liu Z, Manikandan VS, Chen A (2019) Recent advances in nanomaterial-based electrochemical sensing of nitric oxide and nitrite for biomedical and food research. *Curr Opin Electrochem* 16:127–133. <https://doi.org/10.1016/j.coelec.2019.05.013>
93. Cheng C, Zhang Y, Chen H et al (2023) Reduced graphene oxide-wrapped La(0.8)Sr(0.2)MnO(3) microspheres sensing electrode for highly sensitive nitrite detection. *Talanta* 260:124644. <https://doi.org/10.1016/j.talanta.2023.124644>
94. Magri A, Petriccione M, Gutierrez TJ (2021) Metal-organic frameworks for food applications: a review. *Food Chem* 354:129533. <https://doi.org/10.1016/j.foodchem.2021.129533>
95. Wang C, Liu D, Xie Z et al (2014) Functional metal-organic frameworks via ligand doping: influences of ligand charge and steric demand. *Inorg Chem* 53(3):1331–1338. <https://doi.org/10.1021/ic402015q>
96. Lu W, Wei Z, Gu ZY et al (2014) Tuning the structure and function of metal-organic frameworks via linker design. *Chem Soc Rev* 43(16):5561–5593. <https://doi.org/10.1039/c4cs00003j>
97. Zhang W, Li X, Ding X et al (2023) Progress and opportunities for metal-organic framework composites in electrochemical sensors. *RSC Adv* 13(16):10800–10817. <https://doi.org/10.1039/d3ra00966a>
98. Zou D, Liu D (2019) Understanding the modifications and applications of highly stable porous frameworks via UiO-66. *Mater Today Chem* 12:139–165. <https://doi.org/10.1016/j.mtchem.2018.12.004>
99. Feng L, Hou HB, Zhou H (2020) UiO-66 derivatives and their composite membranes for effective proton conduction. *Dalton Trans* 49(47):17130–17139. <https://doi.org/10.1039/d0dt03051a>
100. Yao M-S, Li W-H, Xu G (2021) Metal-organic frameworks and their derivatives for electrically-transduced gas sensors. *Coord Chem Rev* 426:213479. <https://doi.org/10.1016/j.ccr.2020.213479>
101. Cheng D, Li X, Qiu Y et al (2017) A simple modified electrode based on MIL-53(Fe) for the highly sensitive detection of hydrogen peroxide and nitrite. *Anal Methods* 9(13):2082–2088. <https://doi.org/10.1039/c6ay03164a>
102. Zhao Y, Jiang L, Shanguan L et al (2018) Synthesis of porphyrin-based two-dimensional metal-organic framework nanodisk with small size and few layers. *J Mater Chem A* 6(6):2828–2833. <https://doi.org/10.1039/c7ta07911g>
103. Amali RKA, Lim HN, Ibrahim I et al (2022) A copper-based metal-organic framework decorated with electrodeposited Fe(2)O(3) nanoparticles for electrochemical nitrite sensing. *Mikrochim Acta* 189(9):356. <https://doi.org/10.1007/s00604-022-05450-y>
104. Zhang H-J, Chen W-Y, Zou X et al (2022) A novel copper-functionalized MOF modified composite electrode for high-efficiency detection of nitrite and histamine. *J Electrochem Soc* 169(7):077511. <https://doi.org/10.1149/1945-7111/ac8078>
105. Lu S, Jia H, Hummel M et al (2021) Two-dimensional conductive phthalocyanine-based metal-organic frameworks for electrochemical nitrite sensing. *RSC Adv* 11(8):4472–4477. <https://doi.org/10.1039/d0ra10522h>
106. Arul P, Gowthaman NSK, John SA et al (2020) Ultrasonic assisted synthesis of size-controlled Cu-metal-organic framework decorated graphene oxide composite: sustainable electrocatalyst for the trace-level determination of nitrite in environmental water samples. *ACS Omega* 5(24):14242–14253. <https://doi.org/10.1021/acsomega.9b03829>
107. Suma BP, Pandurangappa M (2020) Hydrothermal synthesis of Zr-amino terephthalate and its composite with MWCNTs as a novel electrode material in nitrite quantification. *Electroanalysis* 32(11):2493–2502. <https://doi.org/10.1002/elan.202060091>
108. Gao F, Tu X, Yu Y et al (2022) Core-shell Cu@C@ZIF-8 composite: a high-performance electrode material for electrochemical sensing of nitrite with high selectivity and sensitivity. *Nanotechnology* 33(22):225501. <https://doi.org/10.1088/1361-6528/ac3da7>
109. Yang Z, Zhou X, Yin Y et al (2022) Metal-organic framework derived rod-like Co@carbon for electrochemical detection of nitrite. *J Alloys Compd* 911:164915. <https://doi.org/10.1016/j.jallcom.2022.164915>
110. Zhang W, Ge C-Y, Jin L et al (2021) Nickel nanoparticles incorporated Co, N co-doped carbon polyhedron derived from core-shell ZIF-8@ZIF-67 for electrochemical sensing of nitrite. *J Electroanal Chem* 887:115163. <https://doi.org/10.1016/j.jelechem.2021.115163>
111. Wang K, Wu C, Wang F et al (2018) In-situ insertion of carbon nanotubes into metal-organic frameworks-derived  $\alpha$ -Fe<sub>2</sub>O<sub>3</sub> polyhedrons for highly sensitive electrochemical detection of nitrite. *Electrochim Acta* 285:128–138. <https://doi.org/10.1016/j.electacta.2018.07.228>
112. Dong S, Li Z, Fu Y et al (2020) Bimetal-organic framework Cu-Ni-BTC and its derivative CuO@NiO: construction of three environmental small-molecule electrochemical sensors. *J Electroanal Chem* 858:113785. <https://doi.org/10.1016/j.jelechem.2019.113785>
113. Feng L, Zou M, Lv X et al (2022) Facile synthesis of ZIF-67C@RGO/NiNPs nanocomposite for electrochemical non-enzymatic sensing platform of nitrite. *Microchem J* 179:107508. <https://doi.org/10.1016/j.microc.2022.107508>
114. Zhou X, Zhou Y, Hong Z et al (2018) Magnetic Co@carbon nanocages for facile and binder-free nitrite sensor. *J Electroanal Chem* 824:45–51. <https://doi.org/10.1016/j.jelechem.2018.07.038>
115. Zhe T, Shen S, Li F et al (2023) Bimetallic-MOF-derived crystalline-amorphous interfacial sites for highly efficient nitrite sensing. *Food Chem* 402:134228. <https://doi.org/10.1016/j.foodchem.2022.134228>
116. Arul P, Huang S-T, Mani V et al (2021) Ultrasonic synthesis of bismuth-organic framework intercalated carbon nanofibers: a dual electrocatalyst for trace-level monitoring of nitro hazards. *Electrochim Acta* 381:138280. <https://doi.org/10.1016/j.electacta.2021.138280>

117. Ambaye AD, Muchindu M, Jijana A et al (2023) Screen-printed electrode system based on carbon black/copper-organic framework hybrid nanocomposites for the electrochemical detection of nitrite. *Mater Today Commun* 35:105567. <https://doi.org/10.1016/j.mtcomm.2023.105567>
118. Salagare S, Shivappa Adarakatti P, Venkataramanappa Y (2020) Designing and construction of carboxyl functionalised MWCNTs/Co-MOFs-based electrochemical sensor for the sensitive detection of nitrite. *Int J Environ Anal Chem* 102(17):5301–5320. <https://doi.org/10.1080/03067319.2020.1796989>
119. Sivakumar M, Muthukutty B, Chen T-W et al (2022) Electrocatalytic detection of noxious antioxidant diphenylamine in fruit samples with support of Cu@nanoporous carbon modified sensor. *Chemosphere* 292:133400. <https://doi.org/10.1016/j.chemosphere.2021.133400>
120. Zhao Y, Liu B, Pan L et al (2013) 3D nanostructured conductive polymer hydrogels for high-performance electrochemical devices. *Energy Environ Sci* 6(10):2856–2870. <https://doi.org/10.1039/c3ee40997j>
121. Schiffer L, Shirsath AV, Raël S et al (2022) Electrochemical pressure impedance spectroscopy for polymer electrolyte membrane fuel cells: a combined modeling and experimental analysis. *J Electrochem Soc* 169(3):034503. <https://doi.org/10.1149/1945-7111/ac55cd>
122. Xu M, Zhang H, Zheng J (2022) Polypyrrole microsphere modified porous UiO-66 for electrochemical nitrite sensing. *J Electrochem Soc* 169(4):047515. <https://doi.org/10.1149/1945-7111/ac644c>
123. Li X, Akagi M (2019) Improving multilingual speech emotion recognition by combining acoustic features in a three-layer model. *Speech Comm* 110:1–12. <https://doi.org/10.1016/j.specom.2019.04.004>
124. Mali SM, Narwade SS, Navale YH et al (2019) Facile synthesis of highly porous CuO nanoplates (NPs) for ultrasensitive and highly selective nitrogen dioxide/nitrite sensing. *RSC Adv* 9(10):5742–5747. <https://doi.org/10.1039/c8ra09299k>
125. Manibalan G, Murugadoss G, Hazra S et al (2022) A facile synthesis of Sn-doped CeO<sub>2</sub> nanoparticles: high performance electrochemical nitrite sensing application. *Inorg Chem Commun* 135:109096. <https://doi.org/10.1016/j.inoche.2021.109096>
126. Chen L, Zheng J (2022) Two-step hydrothermal and ultrasound-assisted synthesis of CB/NiCo<sub>2</sub>S<sub>4</sub>@CeO<sub>2</sub> composites for high-sensitivity electrochemical detection of nitrite. *Microchem J* 181:107717. <https://doi.org/10.1016/j.microc.2022.107717>
127. Cheng Z, Song H, Zhang X et al (2022) Non-enzymatic nitrite amperometric sensor fabricated with near-spherical ZnO nanomaterial. *Colloids Surf B: Biointerfaces* 211:112313. <https://doi.org/10.1016/j.colsurfb.2021.112313>
128. Qiu Y, Qu K (2022) Binary organic-inorganic nanocomposite of polyaniline-MnO(2) for non-enzymatic electrochemical detection of environmental pollutant nitrite. *Environ Res* 214(Pt 3):114066. <https://doi.org/10.1016/j.envres.2022.114066>
129. Li Y, Wang T, Wang T et al (2022) Copper oxide nanoleaves covered with loose nickel oxide nanoparticles for sensitive and selective non-enzymatic nitrite sensors. *Mater Res Bull* 149:111712. <https://doi.org/10.1016/j.materresbull.2021.111712>
130. Zhe T, Li M, Li F et al (2022) Integrating electrochemical sensor based on MoO(3)/Co(3)O(4) heterostructure for highly sensitive sensing of nitrite in sausages and water. *Food Chem* 367:130666. <https://doi.org/10.1016/j.foodchem.2021.130666>
131. Shivakumar M, Manjunatha S, Nithyayini KN et al (2021) Electrocatalytic detection of nitrite at NiCo<sub>2</sub>O<sub>4</sub> nanotapes synthesized via microwave-hydrothermal method. *J Electroanal Chem* 882:115016. <https://doi.org/10.1016/j.jelechem.2021.115016>
132. Zhe T, Li R, Wang Q et al (2020) In situ preparation of FeSe nanorods-functionalized carbon cloth for efficient and stable electrochemical detection of nitrite. *Sensors Actuators B Chem* 321:128452. <https://doi.org/10.1016/j.snb.2020.128452>
133. Wang X, Li M, Yang S et al (2020) A novel electrochemical sensor based on TiO<sub>2</sub>-Ti<sub>3</sub>C<sub>2</sub>TX/CTAB/chitosan composite for the detection of nitrite. *Electrochim Acta* 359:136938. <https://doi.org/10.1016/j.electacta.2020.136938>
134. Lu S, Hummel M, Wang X et al (2020) Communication—in situ electrodeposition of nickel phosphide on Ni foam for non-enzymatic detection of nitrite. *J Electrochem Soc* 167(14):146517. <https://doi.org/10.1149/1945-7111/abc99d>
135. Ahammad AJS, Pal PR, Shah SS et al (2019) Activated jute carbon paste screen-printed FTO electrodes for nonenzymatic amperometric determination of nitrite. *J Electroanal Chem* 832:368–379. <https://doi.org/10.1016/j.jelechem.2018.11.034>
136. Dai Y, Huang J, Zhang H et al (2019) Highly sensitive electrochemical analysis of tunnel structured MnO<sub>2</sub> nanoparticle-based sensors on the oxidation of nitrite. *Sensors Actuators B Chem* 281:746–750. <https://doi.org/10.1016/j.snb.2018.11.014>
137. Sha R, Gopalakrishnan A, Sreenivasulu KV et al (2019) Template-cum-catalysis free synthesis of  $\alpha$ -MnO<sub>2</sub> nanorods-hierarchical MoS<sub>2</sub> microspheres composite for ultra-sensitive and selective determination of nitrite. *J Alloys Compd* 794:26–34. <https://doi.org/10.1016/j.jallcom.2019.04.251>
138. Vishnu N, Badhulika S (2019) Single step synthesis of MoSe<sub>2</sub>-MoO<sub>3</sub> heterostructure for highly sensitive amperometric detection of nitrite in water samples of industrial areas. *Electroanalysis* 31(12):2410–2416. <https://doi.org/10.1002/elan.201900310>
139. Sun C, Pan W, Zheng D et al (2019) An electrochemical sensor for nitrite using a glassy carbon electrode modified with Cu/CBSA nanoflower networks. *Anal Methods* 11(39):4998–5006. <https://doi.org/10.1039/c9ay01544b>
140. Nithyayini KN, Harish MNK, Nagashree KL (2019) Electrochemical detection of nitrite at NiFe<sub>2</sub>O<sub>4</sub> nanoparticles synthesized by solvent deficient method. *Electrochim Acta* 317:701–710. <https://doi.org/10.1016/j.electacta.2019.06.026>
141. Ma Y, Wang Y, Xie D et al (2018) NiFe-layered double hydroxide nanosheet arrays supported on carbon cloth for highly sensitive detection of nitrite. *ACS Appl Mater Interfaces* 10(7):6541–6551. <https://doi.org/10.1021/acsami.7b16536>
142. Balasubramanian P, Settu R, Chen S-M et al (2018) A new electrochemical sensor for highly sensitive and selective detection of nitrite in food samples based on sonochemical synthesized calcium ferrite (CaFe<sub>2</sub>O<sub>4</sub>) clusters modified screen printed carbon electrode. *J Colloid Interface Sci* 524:417–426. <https://doi.org/10.1016/j.jcis.2018.04.036>
143. Sudha V, Mohanty SA, Thangamuthu R (2018) Facile synthesis of Co<sub>3</sub>O<sub>4</sub> disordered circular sheets for selective electrochemical determination of nitrite. *New J Chem* 42(14):11869–11877. <https://doi.org/10.1039/c8nj02639d>
144. Manibalan G, Murugadoss G, Thangamuthu R et al (2018) Enhanced electrochemical supercapacitor and excellent amperometric sensor performance of heterostructure CeO<sub>2</sub>-CuO nanocomposites via chemical route. *Appl Surf Sci* 456:104–113. <https://doi.org/10.1016/j.apsusc.2018.06.071>
145. Saravanan J, Ramasamy R, Annal Therese H et al (2017) Electrospun CuO/NiO composite nanofibers for sensitive and selective non-enzymatic nitrite sensors. *New J Chem* 41(23):14766–14771. <https://doi.org/10.1039/c7nj02073b>
146. Jaiswal N, Tiwari I, Foster CW et al (2017) Highly sensitive amperometric sensing of nitrite utilizing bulk-modified MnO<sub>2</sub> decorated Graphene oxide nanocomposite screen-printed electrodes. *Electrochim Acta* 227:255–266. <https://doi.org/10.1016/j.electacta.2017.01.007>
147. Lu S, Yang C, Nie M (2017) Hydrothermal synthesized urchin-like nickel-cobalt carbonate hollow spheres for sensitive

- amperometric detection of nitrite. *J Alloys Compd* 708:780–786. <https://doi.org/10.1016/j.jallcom.2017.03.059>
148. Wang H, Chen P, Wen F et al (2015) Flower-like Fe<sub>2</sub>O<sub>3</sub>@MoS<sub>2</sub> nanocomposite decorated glassy carbon electrode for the determination of nitrite. *Sensors Actuators B Chem* 220:749–754. <https://doi.org/10.1016/j.snb.2015.06.016>
149. Bharath G, Madhu R, Chen S-M et al (2015) Solvent-free mechanochemical synthesis of graphene oxide and Fe<sub>3</sub>O<sub>4</sub>-reduced graphene oxide nanocomposites for sensitive detection of nitrite. *J Mater Chem A* 3(30):15529–15539. <https://doi.org/10.1039/c5ta03179f>
150. Huang H, Lv L, Xu F et al (2017) PrFeO<sub>3</sub>-MoS<sub>2</sub> nanosheets for use in enhanced electro-oxidative sensing of nitrite. *Mikrochim Acta* 184(10):4141–4149. <https://doi.org/10.1007/s00604-017-2446-2>
151. Zhang Y, Chen P, Wen F et al (2016) Fe<sub>3</sub>O<sub>4</sub> nanospheres on MoS<sub>2</sub> nanoflake: electrocatalysis and detection of Cr(VI) and nitrite. *J Electroanal Chem* 761:14–20. <https://doi.org/10.1016/j.jelechem.2015.12.004>
152. Wang H, Wen F, Chen Y et al (2016) Electrocatalytic determination of nitrite based on straw cellulose/molybdenum sulfide nanocomposite. *Biosens Bioelectron* 85:692–697. <https://doi.org/10.1016/j.bios.2016.05.078>
153. Zhang Y, Chen P, Wen F et al (2016) Construction of polyaniline/molybdenum sulfide nanocomposite: characterization and its electrocatalytic performance on nitrite. *Ionics* 22(7):1095–1102. <https://doi.org/10.1007/s11581-015-1634-5>
154. Puspalak A, Chinnadurai P, Prathibha R, Kumar MP, Manjushree SG, UdayaKumar V, Adarakatti P (2023) Cobalt oxide nanoparticles based carbon electrode for the detection of residual nitrite in the soil of agricultural fields. *Mater Res Innov* 27(2):100–109. <https://doi.org/10.1080/14328917.2022.2085909>
155. Salagare S, Shivappa Adarakatti P, S. B P et al (2022) A selective electrochemical sensor based on titanium dioxide-reduced graphene oxide nanocomposite (TiO<sub>2</sub>-RGO/GCE) for the efficient determination of nitrite. *Mater Res Innov* 27(1):33–44. <https://doi.org/10.1080/14328917.2022.2071013>
156. Wang J, Zhao D, Zhang Y et al (2014) A highly sensitive sensor for the detection of nitrite based on a nanoporous Fe<sub>2</sub>O<sub>3</sub>-CoO composite. *Anal Methods* 6(9):3147–3151. <https://doi.org/10.1039/c4ay00171k>
157. Rahim A, Santos LSS, Barros SBA et al (2014) Electrochemical detection of nitrite in meat and water samples using a mesoporous carbon ceramic SiO<sub>2</sub>/C electrode modified with in situ generated manganese(II) phthalocyanine. *Electroanalysis* 26(3):541–547. <https://doi.org/10.1002/elan.201300468>
158. Li Y, Wang H, Liu X et al (2014) Nonenzymatic nitrite sensor based on a titanium dioxide nanoparticles/ionic liquid composite electrode. *J Electroanal Chem* 719:35–40. <https://doi.org/10.1016/j.jelechem.2014.02.006>
159. Verma S, Arya P, Singh A et al (2020) ZnO-rGO nanocomposite based bioelectrode for sensitive and ultrafast detection of dopamine in human serum. *Biosens Bioelectron* 165:112347. <https://doi.org/10.1016/j.bios.2020.112347>
160. Alam MM, Uddin MT, Asiri AM et al (2020) Fabrication of selective l-glutamic acid sensor in electrochemical technique from wet-chemically prepared RuO<sub>2</sub> doped ZnO nanoparticles. *Mater Chem Phys* 251:123029. <https://doi.org/10.1016/j.matchemphys.2020.123029>
161. Manjari G, Saran S, Radhakrishnan S et al (2020) Facile green synthesis of Ag-Cu decorated ZnO nanocomposite for effective removal of toxic organic compounds and an efficient detection of nitrite ions. *J Environ Manag* 262:110282. <https://doi.org/10.1016/j.jenvman.2020.110282>
162. Yang W, Bai Y, Li Y et al (2005) Amperometric nitrite sensor based on hemoglobin/colloidal gold nanoparticles immobilized on a glassy carbon electrode by a titania sol-gel film. *Anal Bioanal Chem* 382(1):44–50. <https://doi.org/10.1007/s00216-005-3160-1>
163. Manibalan G, Murugadoss G, Thangamuthu R et al (2020) CeO<sub>2</sub>-based heterostructure nanocomposite for electrochemical determination of l-cysteine biomolecule. *Inorg Chem Commun* 113:107793. <https://doi.org/10.1016/j.inoche.2020.107793>
164. Khoshroo A, Hosseinzadeh L, Adib K et al (2021) Earlier diagnoses of acute leukemia by a sandwich type of electrochemical aptasensor based on copper sulfide-graphene composite. *Anal Chim Acta* 1146:1–10. <https://doi.org/10.1016/j.aca.2020.12.007>
165. Radhakrishnan S, Krishnamoorthy K, Sekar C et al (2014) A highly sensitive electrochemical sensor for nitrite detection based on Fe<sub>2</sub>O<sub>3</sub> nanoparticles decorated reduced graphene oxide nanosheets. *Appl Catal B Environ* 148–149:22–28. <https://doi.org/10.1016/j.apcatb.2013.10.044>
166. Salhi O, Ez-zine T, El Rhazi M (2021) Hybrid Materials Based on Conducting Polymers for Nitrite Sensing: A Mini Review. *Electroanalysis* 33(7):1681–1690. <https://doi.org/10.1002/elan.202100033>
167. Janaky C, Visy C (2013) Conducting polymer-based hybrid assemblies for electrochemical sensing: a materials science perspective. *Anal Bioanal Chem* 405(11):3489–3511. <https://doi.org/10.1007/s00216-013-6702-y>
168. Ramanavičius A, Ramanavičienė A, Malinauskas A (2006) Electrochemical sensors based on conducting polymer—polypyrrole. *Electrochim Acta* 51(27):6025–6037. <https://doi.org/10.1016/j.electacta.2005.11.052>
169. Tsai M-D, Wang Y-C, Chen Y-L et al (2022) Selectively confined poly(3,4-ethylenedioxythiophene) in the nanopores of a metal-organic framework for electrochemical nitrite detection with reduced limit of detection. *ACS Appl Nano Mater* 5(9):12980–12990. <https://doi.org/10.1021/acsanm.2c02790>
170. Asiri AM, Adeosun WA, Marwani HM et al (2020) Homopolymerization of 3-aminobenzoic acid for enzyme-free electrocatalytic assay of nitrite ions. *New J Chem* 44(5):2022–2032. <https://doi.org/10.1039/c9nj06058h>
171. Islam T, Hasan MM, Akter SS et al (2019) Fabrication of Ni-Co based heterometallo-supramolecular polymer films and the study of electron transfer kinetics for the nonenzymatic electrochemical detection of nitrite. *ACS Appl Polym Mater* 2(2):273–284. <https://doi.org/10.1021/acsapm.9b00797>
172. Jiao M, Li Z, Li Y et al (2018) Poly(3,4-ethylenedioxythiophene) doped with engineered carbon quantum dots for enhanced amperometric detection of nitrite. *Mikrochim Acta* 185(5):249. <https://doi.org/10.1007/s00604-018-2784-8>
173. Xiao Q, Feng M, Liu Y et al (2017) The graphene/polypyrrole/chitosan-modified glassy carbon electrode for electrochemical nitrite detection. *Ionics* 24(3):845–859. <https://doi.org/10.1007/s11581-017-2247-y>
174. Wang X, Tan W, Ji H et al (2018) Facile electrosynthesis of nickel hexacyanoferrate/poly(2,6-diaminopyridine) hybrids as highly sensitive nitrite sensor. *Sensors Actuators B Chem* 264:240–248. <https://doi.org/10.1016/j.snb.2018.02.171>
175. Shen Y, Zhu G, Yang J et al (2018) Ultrafine copper decorated polypyrrole nanotube electrode for nitrite detection. *Ionics* 25(1):297–307. <https://doi.org/10.1007/s11581-018-2577-4>



176. Qian W, Guo H, Li X et al (2021) An amperometric nitrite sensing platform with enhanced sensitivity based on copper nanoparticle/nanostructured polyaniline hydrogel nanocomposite. *Ionics* 27(12):5297–5308. <https://doi.org/10.1007/s11581-021-04227-2>
177. Li Y, Geng C, Xu X et al (2021) Construction of polythiophene-derivative films as a novel electrochemical sensor for highly sensitive detection of nitrite. *Anal Bioanal Chem* 413(26):6639–6647. <https://doi.org/10.1007/s00216-021-03630-y>

**Publisher's note** Springer Nature remains neutral with regard to jurisdictional claims in published maps and institutional affiliations.

Springer Nature or its licensor (e.g. a society or other partner) holds exclusive rights to this article under a publishing agreement with the author(s) or other rightsholder(s); author self-archiving of the accepted manuscript version of this article is solely governed by the terms of such publishing agreement and applicable law.